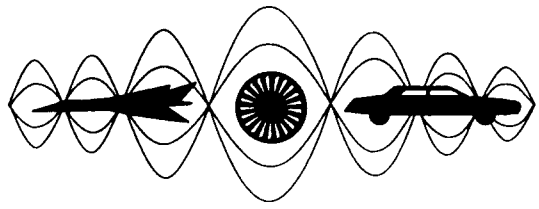

FIFTH INTERNATIONAL CONGRESS ON SOUND AND VIBRATION
DECEMBER 15-18, 1997
ADELAIDE, SOUTH AUSTRALIA

Distinguished Keynote Paper

RECENT DEVELOPMENTS IN ACOUSTICS AND VIBRATION

Malcolm J. Crocker

Department of Mechanical Engineering
Auburn University, AL 36849, USA

Abstract

In recent years there have been rapid advances in digital computers, the miniaturization of electronic circuits and the development of new materials. In the acoustics and vibration fields these advances have led to a continual increase in computational power and speed, improved acoustics and vibration transducers and instrumentation and better measurement techniques. In many cases the developments have been synergistic; new experimental knowledge has led to improved theoretical models and approaches and vice versa. Improved computers have allowed the development of a host of computer programs and increasing numbers have become available as commercial acoustics and vibration software. Of particular importance has been the development of numerical calculation schemes such as the finite element method (FEM) and the boundary element method (BEM) which have led to much improved predictive capabilities in many fields. However, advances have been in many other areas of acoustics as well and not confined just to such numerical prediction schemes. As examples, a few of these advances will be concisely summarized including: increased knowledge of and use of FEM and BEM, Computational Aeroacoustics, Sonochemistry, Thermoacoustic Engines, Active Noise and Vibration Control, Sound Intensity Measurements and their uses, Techniques of Speech Coding and Recognition of Speech, Ultrasonics in Medical Diagnostics, and Cochlear Mechanics.

1.0 INTRODUCTION

The development of the digital computer in the 1950's signaled the beginning of increasingly rapid developments in science. Even the early digital computers enabled rapid calculations and analytical solutions of problems to be made that were previously insoluble because of the enormous amount of calculations and thus time and manpower needed for their solution. Further developments in digital computers have continued this trend enabling ever more rapid

and massive calculations and solutions of problems of increasing complexity. The developments have also brought lower costs and miniaturization of components and the late 1970's also saw the development of the desktop and portable computers that put computing power into the hands of increasing numbers of scientists. These trends have continued unabated to the present day. In fact the established trend may even accelerate. Moore's law which for the last 30 years has predicted very accurately that the amount of memory that could be stored on a computer chip (and thus its speed and efficiency) doubled every 18 months recently seems to be violated. On 17 September 1997, Intel announced a new chip that uses multilevel cell flash memory. In less than a week on 21 September 1997, I.B.M. announced that it had solved a fundamental problem holding back the development of faster semiconductor chips and that early in 1998 it will begin manufacturing chips that are smaller and up to 40% faster than the most advanced chips currently being produced commercially. Such rapid advances in computer technology may lead to a doubling of chip performance every nine instead of eighteen months as predicted by Moore's law. Such rapid developments in computer power (and the attendant reduction in cost) have had dramatic effects on the solution of acoustics and vibration problems. Some very visible results have been the development of the finite element method (FEM) and the boundary element method (BEM) that can solve complicated acoustics and vibration problems and of increasing numbers of software programs that can run on mainframe and more and more on desktop and portable computers. Digital computers have also increasingly been built into instrumentation and analysis equipment enabling more sophisticated experimentation in acoustics and vibration and more rapid and sophisticated analysis of the results. The development of piezoelectric materials has also led to advances in the design of acoustics and vibration transducers. All these and other developments have had a synergistic effect and have enabled or aided advances in several fields of acoustics and vibration. Some of these are outlined in the following.

2.0 NUMERICAL APPROACHES: FINITE ELEMENTS AND BOUNDARY ELEMENTS

In cases where the geometry of a vibrating structure or an acoustic space is complicated and where lumped element or modal approaches cannot be used, then it is necessary to use numerical approaches. In the late 1960's with the advent of powerful digital computers, the finite element method (FEM) became feasible. Finite element approaches were first used to analyze static and then dynamic (vibration) structural problems. [1] Later FEM was used with acoustics problems. In this approach the fluid is divided into a number of small fluid elements (usually rectangular or triangular) and the equations of motion are solved for the elements, ensuring that the sound pressure and volume velocity are continuous at the node points where the elements are joined. The FEM has been widely used to study the acoustical performance of automobile cabins, muffler systems and aircraft problems. [2-6]. Figures 1, 2 and 3 show the transmission loss (TL) of a reverse flow muffler predicted by one of the first FEM programmes designed by the author and his colleagues in the early 1970's. Such FEM programmes are now widely available from commercial software companies. The TL of mufflers comprised of combinations of side in-centre out (SI-CO), centre in-side out (CI-SO), and side in-side out (SI-SI) reversing chambers and Helmholtz resonators is shown in these figures. Craggs has given a good recent review of the use of FEM in acoustics.[2] Regular (e.g. triangular or rectangular) elements have limited use in practice, but can be transformed into irregular elements that are more useful.[2] (see Fig. 4). Element matrices can be formed with 20 or 32 nodes instead of the simpler 8-node elements. Figure 5 shows a cavity

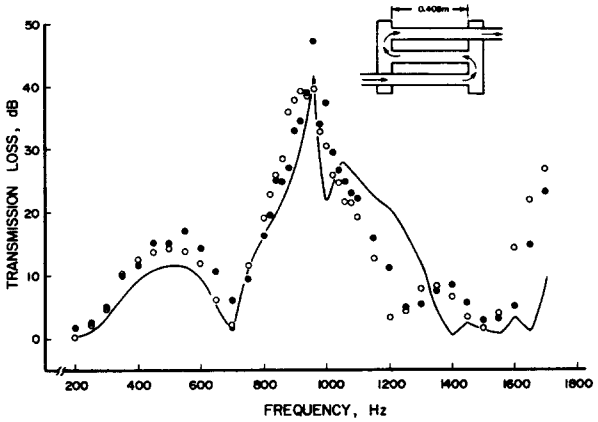

Figure 1 — Transmission loss characteristics for combination of SI-CO and CI-SO flow-reversing chambers ——— is predicted; o is measured without flow; and • is measured with a flow speed of 32 m/s [4]

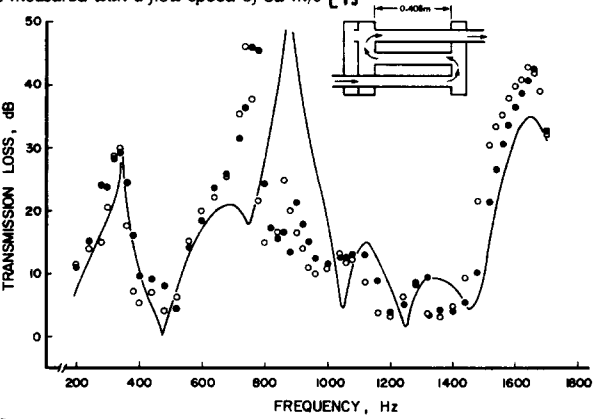

Figure 2 — Transmission loss characteristics for combination of SI-CO and CI-SO flow-reversing chambers ——— is predicted; o is measured without flow; and • is measured with a flow speed of 32 m/s [4]

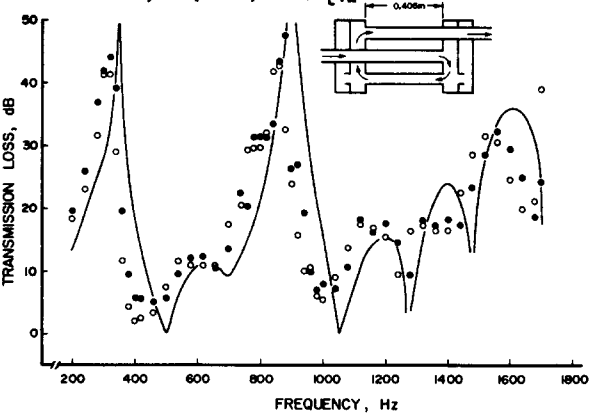

Figure 3 — Transmission loss characteristics for combination of CI-SO and SI-SO flow-reversing chambers with two resonators ——— is predicted; o is measured without flow; and • is measured with a flow speed of 32 m/s [4]

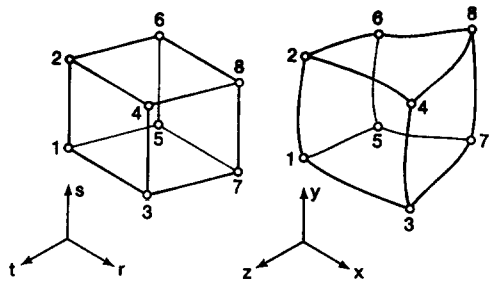

Fig. 4 Transformation from a regular rectangular element in r, s, t to an irregular element in x, y, z.

representing that of an automobile (car) interior. In a recent study thirty 32-node elements were used resulting in a system with 378 degrees of freedom. A comparison of predicted and measured natural frequencies for the cavity in Fig. 5) is given in Table 1.

The boundary element method was developed a little later than the FEM. In the BEM approach the elements are described on the boundary surface only, which reduces the computational dimensions of the problem by one. This correspondingly produces a smaller system of equations than the FEM and thus saves computational time considerably because of the use of a surface mesh instead of a volume mesh. For sound propagation problems involving the radiation of sound to infinity, the BEM is more suitable because the radiation condition at infinity can be easily satisfied with the BEM, unlike with the FEM. However, the FEM is better suited than the BEM for the determination of the natural frequencies and mode shapes of cavities or where the response at a large number of frequencies must be evaluated. Seybert and Wu have discussed the use of BEM in acoustics problems in a recent review. [7]

Figure 6 shows a boundary element mesh model for the sound radiated from a tire touching the hard reflecting ground plane together with the contours of the sound pressure levels (SPL) radiated by the tire at 100 Hz. [7] Figure 7 shows a boundary element mesh used for a simple expansion chamber muffler. After the mesh shown is created by the user (with element size no larger than a certain fraction of the acoustic wavelength) the boundary condition information at every node is supplied to the BEM. The BEM is used to calculate the sound pressure on the inner surface of the cavity as well as at field points inside the cavity. (See Fig. 7). The transmission loss (TL) both calculated using the BEM (solid line) and measured experimentally (triangles) is shown in Fig. 8. [7] The BEM results were obtained by specifying the velocity at all of the node points to be zero (since the muffler casing was assumed to be rigid) except for the nodes at the inlet and exit of the muffler. At the inlet, the velocity was specified to be unity and at the outlet the boundary condition was that the acoustic impedance was equal to the characteristic impedance of the medium. Figure 7 shows the contours of equal sound pressure level (SPL) at 2900 Hz, a frequency at which the TL is approximately zero (see Fig. 8). Figure 7 shows that there is a cross mode at this frequency resulting in the poor TL.

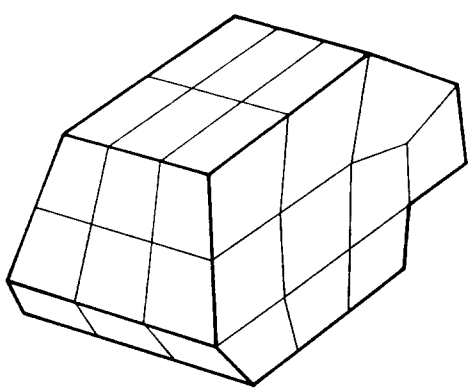

Fig. 5 Acoustic finite element grid for a model car enclosure. Assembly is of the 32-node isoparametric elements.

TABLE 1 Natural Frequencies of Irregular Cavity

Mode	Finite Element Simulation	Measured Frequency
100	140.8	154.6
001	160.3	168.2
010	208.9	220.2
200	243.3	251.0
101	267.8	281.8
201	288.8	301.8
110	299.9	312.2
110	299.9	312.2
002	315.4	323.8
102	353.2	355.4
111	347.0	366.6
020	371.3	378.2

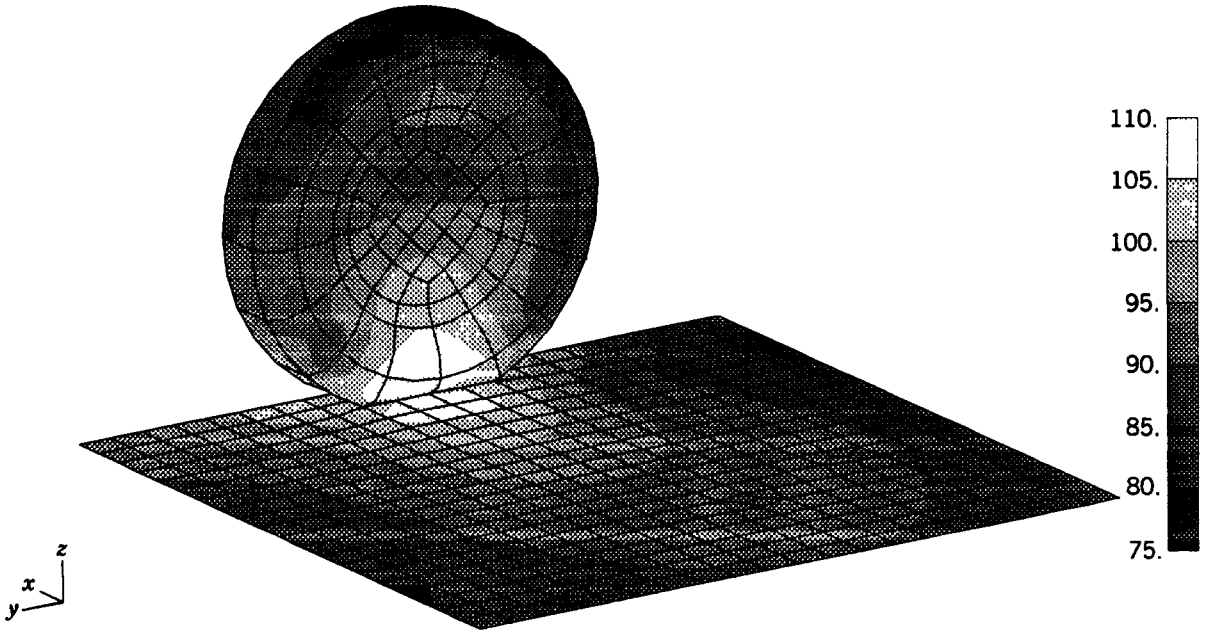

Fig. 6 The SPL contour plot of tire radiation at 1000 Hz.

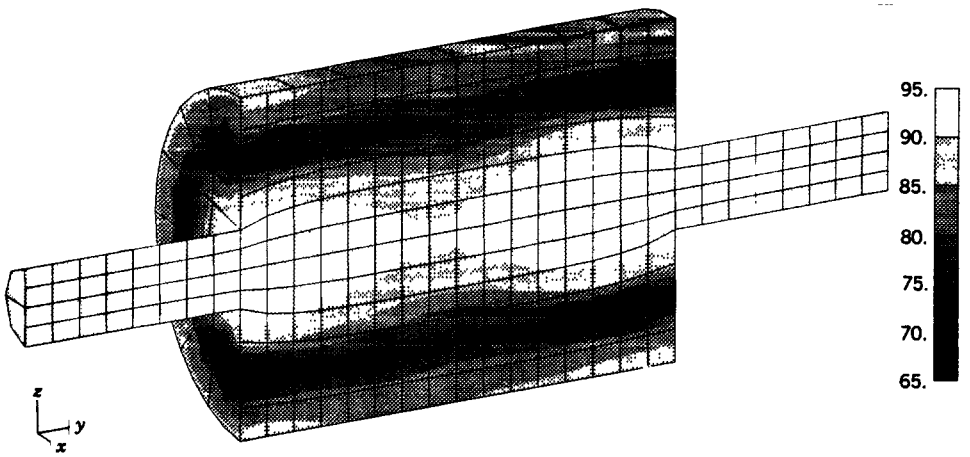

Fig. 7 The SPL contour plot for the expansion chamber muffler at 2900 Hz.

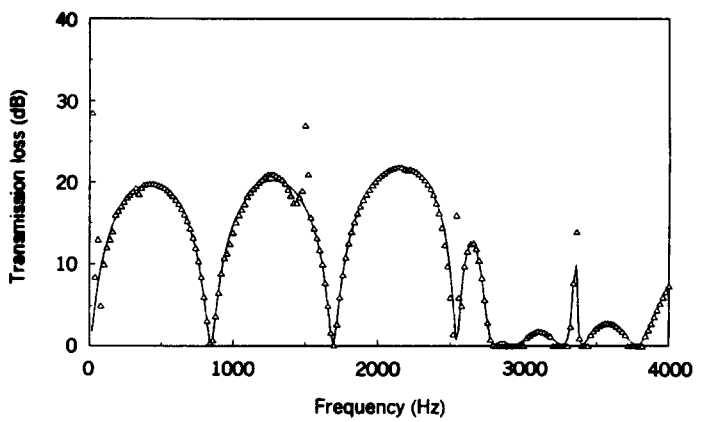

Fig. 8 The TL for the simple expansion chamber muffler: solid line, BEM; symbols, experiment.

In the last decade, FEM and BEM commercial software have become widely available. Recently the FEM and BEM approaches have been combined to obtain a powerful tool for the solution of vibro-acoustic problems. This approach is sometimes known as BFEM. [8,9] With BFEM, normally FEM is used for modeling the vibration response of a structure and BEM for modeling the sound radiation into the fluid. Hamadi has recently reviewed several applications of this modeling which is conveniently undertaken with the computational capabilities of modern workstations and super-computers. [8] For example Fig. 9a shows a numerical model of the ARIANE 5 space launcher. Figure 9b shows a qualification test of the ARIANE fairing. Figure 9c shows a comparison between the experimental results for the sound pressure levels (SPL) averaged over 20 microphones placed around the fairing and predictions using BFEM. Figure 9d shows the *noise reduction factor* of the fairing. [8]

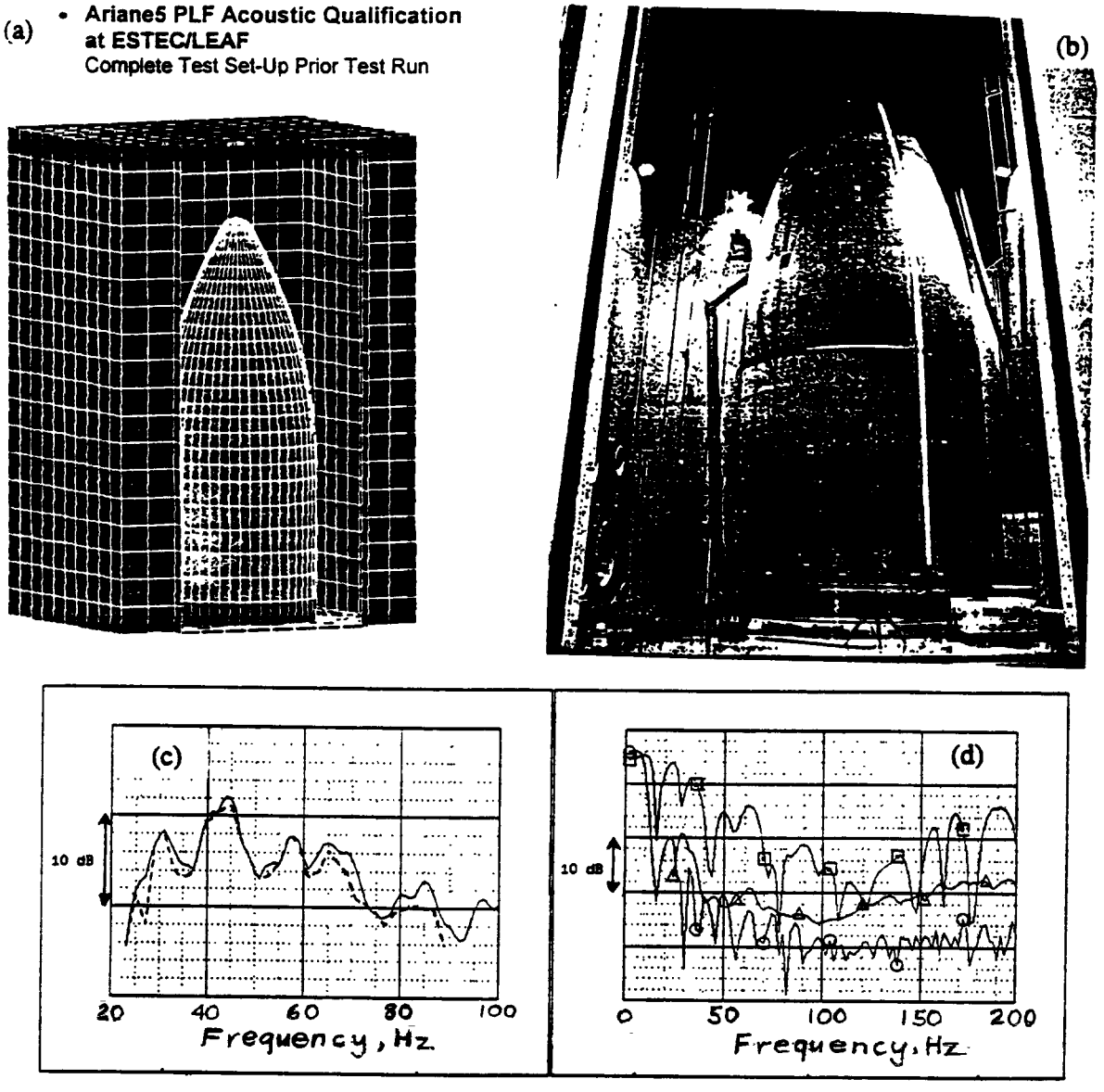

Fig. 9 Space applications :
a) RAYON numerical model
b) Qualification test of ARIANE fairing
c) Averaged SPL
——— (test mean ext.noise)
– – – – – (Rayon mean ext. noise)
d) Noise Reduction factor of the fairing
—○— Air (diffuse)
—□— Helium (95%)
—△— SAA (35%)

3.0 COMPUTATIONAL AEROACOUSTICS

Although both classical modal approaches and the FEM and BEM are useful in solving a variety of complicated acoustic problems it is difficult to include the effects of either mean or unsteady fluid flow in these approaches. Recently digital computers have also become useful in predicting sound propagation in flowing fluid media. [9-13] There are several possible approaches.

In one approach the Navier Stokes equations for flow are used in a time marching scheme to obtain a steady state solution. The unknown variables are the fluid density, fluid velocity components, and the total fluid energy. The components of the viscous stress tensor and the heat flux vector are computed from flow variables. [11] In order to derive the equations that govern the acoustic disturbances in the flow, the unknown fluid variables are decomposed into mean or steady flow components and acoustic perturbation components. By subtracting the equation governing the mean flow from the full fluid dynamic equation, a set of hyperbolic nonlinear equations governing acoustic disturbances in a viscous compressible flow is obtained. There are no exact analytical solutions to these equations and it is necessary to linearize them. The nonlinear equations are linearized by neglecting products of acoustic variables. In order to solve the equations numerically, a consistent set of boundary conditions needs to be prescribed. Boundary conditions for flow duct acoustics have been formalized for some ideal cases, such as hard-walled ducts where it can be assumed that the normal velocity at the wall is zero. The inflow and outflow and the wall boundary conditions need to be considered separately (as in the FEM and BEM formulations discussed before). However in the FEM and BEM formulations it is possible to use impedance conditions (ratio of sound pressure to velocity) because the formulation is in the frequency domain. However computational acoustics is carried out in the time domain. This causes complications with the boundary conditions at the walls of absorbing ducts (where the sound pressure and velocity must be prescribed separately and impedance concepts cannot be used, because the formulation is necessarily in the time domain.)

Another approach in aeroacoustics is followed by Lilley et al. [9] This includes the solution of the complete compressible Navier Stokes equations at low Reynolds numbers using methods based on Lighthill's acoustic analogy. In this approach the characteristics of the unsteady flow have been obtained from a reduced form of the Navier Stokes equations in which the time dependent large scale turbulent structure is derived. This method requires the turbulence modeling of the small scale turbulent structure which is not resolved on the calculations. The flow equations are solved using a time marching algorithm with non-reflecting boundary conditions applied to the computational domain. The calculated flow field is compared with experimental results showing that the large scale structure is resolved adequately in the

calculations. One numerical example from the work of Zhang et al. [14] is shown in Fig. 10 for a self-excited cavity at M = 1.5. The results may be compared with the experimental results of Zhang and Edwards [15] shown in Fig. 11. Satisfactory qualitative agreement is seen. From the calculated data base for the large scale structure, the space-retarded time co-variance of Lighthill's stress tensor, T_{ij}, can be calculated and from this the far field sound radiation can be found. Good agreement has been found between the calculated and measured data both within and external to the flow in the radiation field. The assumption is made that the sound radiation to the observer obeys linear acoustic propagation.

Figure10 Experimental Interferogram showing shear layer impingement M_∞=1.5 Zhang and Edwards[13].

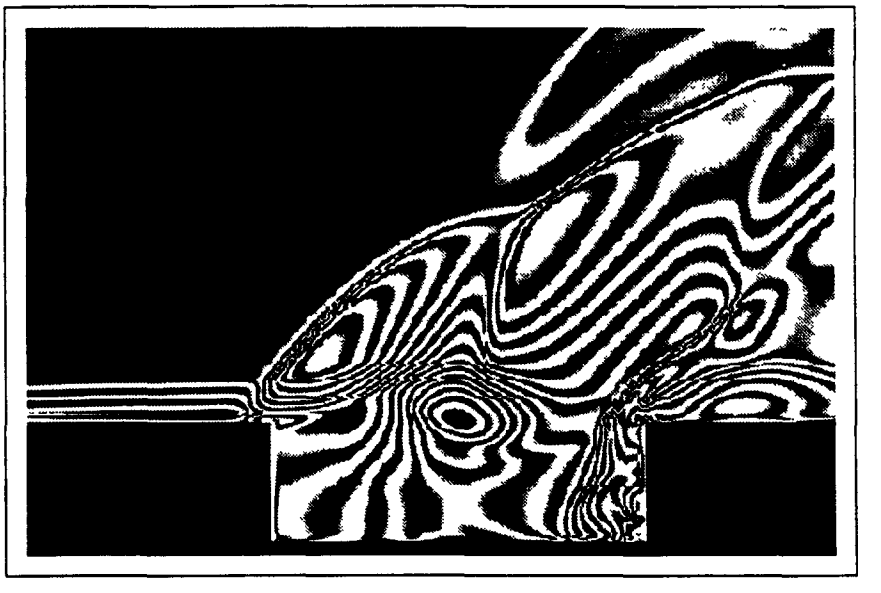

Figure11 Numerical Interferogram M_∞=1.5 showing shear layer impingement Zhang et al.[9]

4.0 ULTRASONICS, SONOCHEMISTRY AND SONOLUMINESCENCE

Chemistry may be regarded as the interaction of energy and matter. Fig 12 shows the interaction of energy, time of interactions and pressure that define different chemical processes. See the recent review by Suslick and Crum. [16] Several other recent reviews and books are useful in understanding these phenomena. [17-24] This figure shows the following forms of chemistry: a) thermal chemistry with medium pressure, time scales and energy, and b) piezo-chemistry which is characterized by high pressure, long time-scales and low energy as found in geological conditions, and c) sonochemistry characterized by high pressure, short time scales and medium to high energy. All these forms of chemistry are related although each has its own individual characteristics. Of main interest to our discussion here is sonochemistry and sonoluminescence and they are now briefly described. [16-23]

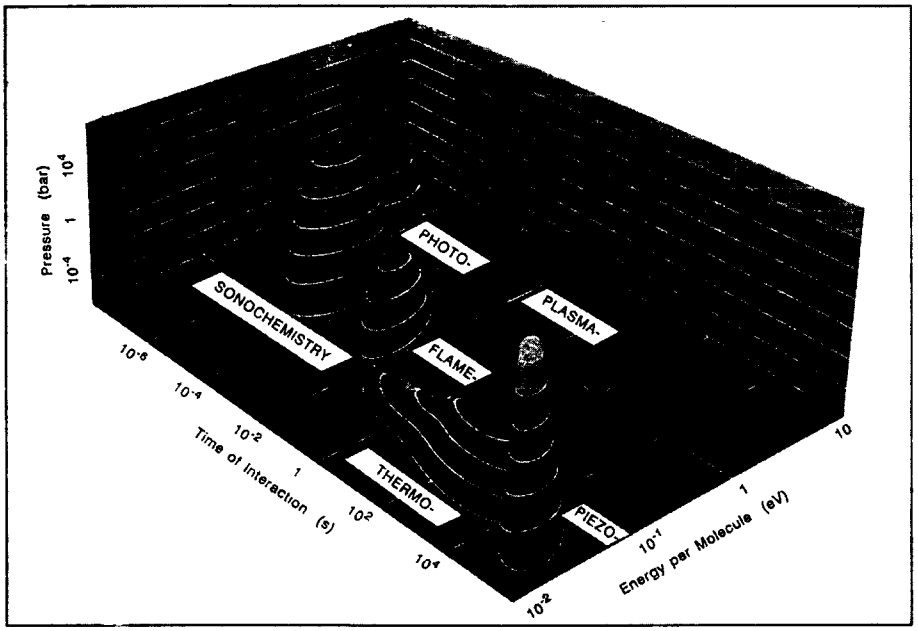

Figure 12. Islands of chemistry as a function of time, pressure, and energy. Adapted from "The Chemical Effects of Ultrasound," by Kenneth S. Suslick. Copyright © 1989 by Scientific American Inc.

During the ultrasonic irradiation of liquids, high energy chemical reactions can occur. The chemical reactions that occur do not, however, come from the direct interaction between the ultrasound waves and the chemical molecules. The speed of sound in most liquids is of the order of 1500 m/s and ultrasonic frequencies span the range of about 15 kilohertz to tens of megahertz resulting in acoustic wavelengths of the order of 10 to 10^{-4} cm. These are not molecular dimensions. Instead when ultrasound passes through a liquid the bubbles can form, grow rapidly and then implode as shown in Figs. 13a, 13b and 13c.

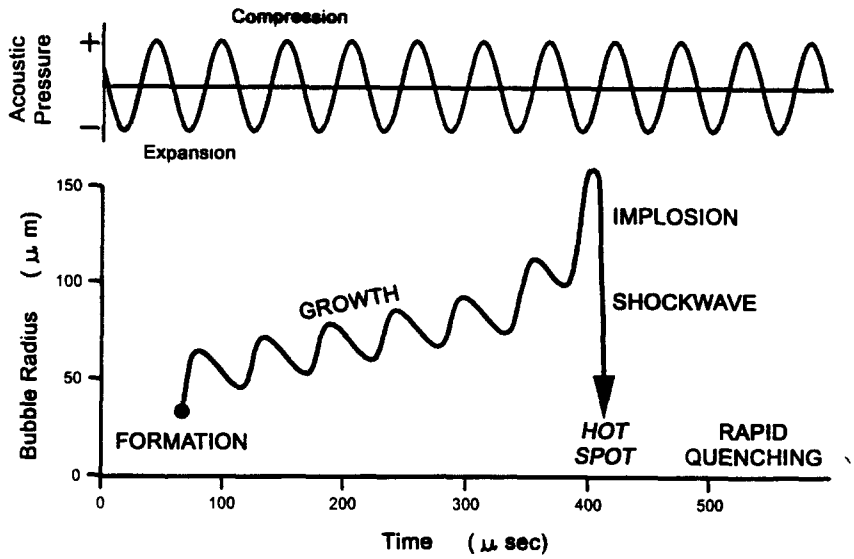

Figure 13a Transient cavitation.

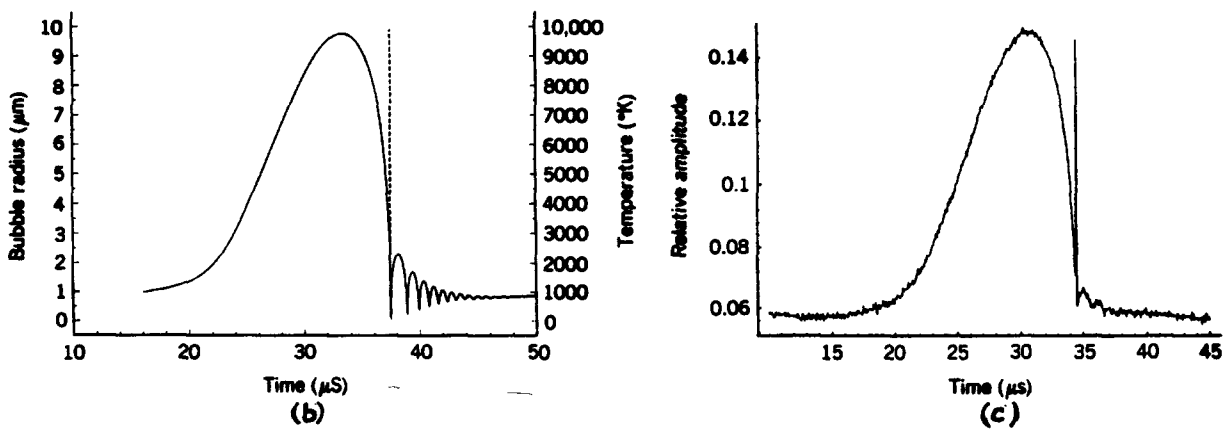

Fig. 13 (b) Theoretical response of a single gas bubble when driven under conditions of SBSL (solid line). Pressure amplitude 0.136 MPa, equilibrium radius 4.5 μm, and driving frequency 26.5 kHz. Bubble expands to several times its initial radius and then implosively collapses. Broken line: calculation of the interior bubble temperature assuming an adiabatic collapse of the cavity contents. (Courtesy of John Allen.) (c) Measured response of a gas bubble to conditions similar to those shown. Experimentally determined bubble radius reconstructed from the square root of the scattered laser light intensity. Intensity spike near bubble collapse is not due to the laser but results from the sonoluminescence emissions. With some minor adjustments, the theoretical and experimental curves for the bubble radius can be made to coincide. (Courtesy of Tom Matula.)

The ultrasound consists of expansion and compression waves. If the sound waves are intense enough, the expansion waves can cause cavities (bubbles) to occur. Then the compression wave compresses the bubble. The next expansion wave re-expands it and so on. The bubble oscillates at the frequency of the sound field and can grow through various mechanisms including rectified diffusion. With this mechanism the surface area after expansion is greater than the surface area after compression and so the bubble grows. The oscillating bubble tends to grow until it reaches a resonant size and condition determined by the sound field. When the bubble is at resonance it is coupled well to the sound field and can readily absorb energy even in a single cycle. After such growth it is no longer coupled well to the sound field. Then the surface tension together with the next compression wave causes an implosive collapse of he bubble in a very short time. During the collapse a shock wave can exist in the bubble gas and very rapid (and almost adiabatic) heating occurs causing enormous localized temperatures and pressures. Local hot spots occur in the liquid and are responsible for rapid chemical changes (sonochemical) and light emission (sonoluminescence).

Ultrasound can be added to liquids as shown in Figure 14. [16] Figure 15 shows the sonoluminescence created by the titanium horn tip of a titanium horn. [17] The temperature created in the hot spots that cause the sonoluminescence is estimated to be about 5000 K.

In addition, ultrasound has recently been found to cause many possible chemical effects, including vast improvements in both stoichiometric and catalytic reactions [16]. Intense radiation by ultrasound has been found to increase reactivity by almost one million times. [16]

The chemical effects of ultrasound can be classified as follows: 1) homogeneous sonochemistry of liquids, 2) heterogeneous sonochemistry of liquid-liquid or liquid-solid systems and 3) sonocatalysis (which overlaps the first two). [16] Chemical reactions do not generally occur with the irradiation of solids or solid-gas systems.

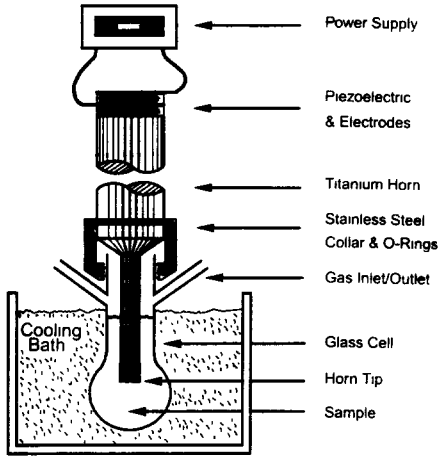

Figure 14 Sonochemical apparatus.

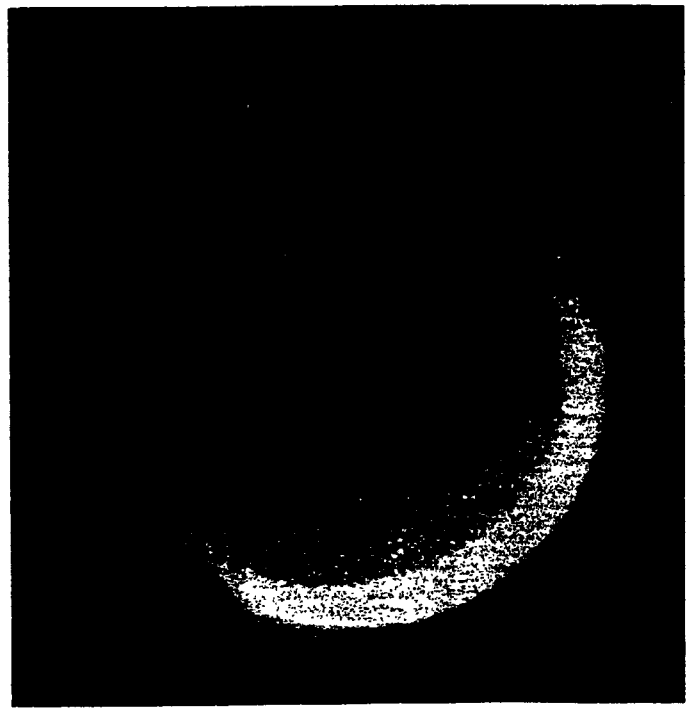

Figure 15 Sonoluminescence from a Vibrating Titanium Rod (1 cm long).

5.0 THERMOACOUSTIC ENGINES

Thermoacoustic engines have recently been shown to be commercially feasible. Such engines use the thermal effects present in sound waves to produce useful acoustic power from the heat inputs or refrigeration from acoustic power. Swift has given good recent reviews of thermoacoustic engines. [25,26] Swift et al. and others have written other such reviews and also discussed details of the design of such systems. [27-33]

The earliest thermoacoustic engine was the Sondhauss tube shown in Figure 16a. Glassblowers in the 19th Century were aware that when a hot glass bulb was being blown on a cool glass tubular section that sound would sometimes be radiated from the stem tip. Lord Rayleigh explained the physics of the phenomenon thus: sound is generated by the oscillatory thermal expansion and contraction of the air in the tube which in turn is due to the acoustic motion of the air towards and away from the heated end of the tube. [34] The Sondhauss tube is a thermoacoustic prime mover and converts heat into mechanical work in the form of sound. It utilizes an acoustic standing wave with the bulb and stem forming a resonator.

Figure 16b shows another example of a standing wave thermoacoustic engine, in this case a thermoacoustic refrigerator. The particular refrigerator shown in Fig 16b has a helium-filled resonator driven by a loudspeaker and containing a stack whose hot heat exchanger is fixed at room temperature. Hofler demonstrated that when this device has a static pressure of 1 MPa and is driven with an amplitude of 30 kPa, its cold heat exchanger reaches a temperature of 200 K. At somewhat higher temperatures it produces 3 W of cooling power with 0.12 of the Carnot efficiency. [35] Figure 16c shows a travelling wave thermoacoustic heat pump.

A major milestone occurred at Cryenco Inc. (Denver, Colorado) in March 1997 when a thermoacoustic refrigerator was used to liquefy natural gas at the rate of 100 gallons a day. This device burned some of the natural gas as a heat source and had a cooling power of 1515 watts. The efficiency of the device was 19% of the Carnot efficiency. The liquefaction was achieved at 115 K (-250 F) and at atmospheric pressure. [36] The advantage of such devices is simplicity of design and maintenance since there are no moving parts. This is a great advantage in liquefying natural gas in field conditions. Further development is underway.

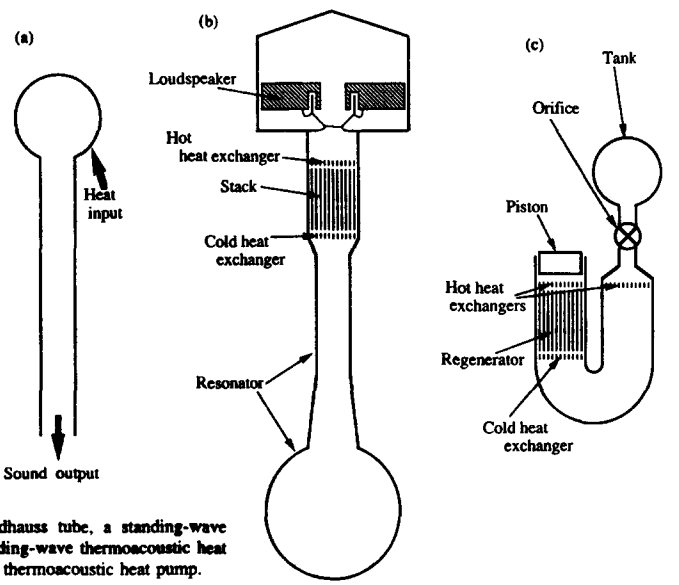

Fig. 16 Examples of thermoacoustic engines: (*a*) the Sondhauss tube, a standing-wave thermoacoustic prime mover; (*b*) Hofler's refrigerator, a standing-wave thermoacoustic heat pump; (*c*) the orifice pulse-tube refrigerator, a traveling-wave thermoacoustic heat pump.

6.0 ACTIVE NOISE AND VIBRATION CONTROL

Passive control of noise and vibration can often be achieved through the use of sound absorption, machine enclosure, acoustic barriers, vibration isolation, vibration damping , etc. However all of these measures normally are ineffective at low frequency. Fortunately this is the frequency region in which active control is easiest to implement successfully. The concept has been known for many years. Even Lord Rayleigh was aware of it. Lueg patented an elementary device for noise control in 1936.[37] However, although there have been quite active research efforts for over 20 years, it is only in the last few years that active control has become commercialized in a few, mostly high technology applications. These include the production of active hearing protectors, the low frequency exhaust muffling of some internal combustion engines, active vibration isolation of machinery such as automobile engines from vehicle bodies, the active control of transformer noise and the active control of the pure tone propeller noise in the cabins of some light and moderate size passenger aircraft. Nelson and Elliott have given a recent review of active noise control [38] and Fuller of active vibration control [39]. Hansen has also surveyed the field of active noise control. [40] Fuller and von Flotow have reviewed both active sound and vibration control [41], and Crawley has surveyed the general field of smart structures of which active control is just one application. [42] A number of books on these fields have appeared in recent years. [43-47]

The advances in active noise and vibration control have become possible for several reasons, but the most important include the recent advances in fast digital signal processing (DSP) computer chips and active control algorithms. In active noise and vibration control systems, secondary inputs are supplied to the system to be controlled in order to modify its response in some desired way. The main components of an active noise or vibration control system include: 1) the *plant*, 2) *sensors*, 3) *actuators*, and 4) *controllers*. The physical system to be controlled is often known as the *plant*. The *sensors* are normally used to detect the *error* in the system (*plant*) response compared with the desired response. The *controllers* are used to implement the control algorithm chosen sending control signals to the *actuators* to modify the system (*plant*) response as desired. [38] There are two main approaches in active noise and vibration control: adaptive feedforward control and adaptive feedback control. Figure 17 gives an illustration of these with the active control of plane wave sound propagating in a duct.

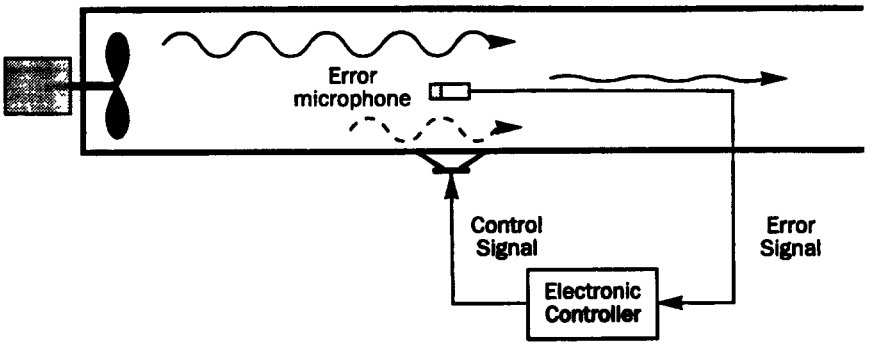

Figure 17 Basic active noise control system.
(a) Feedback system

[40] In Fig. 17a with feedback control, the error microphone senses the sound signal which is then processed by the controller to produce a suitable control signal for the actuator which attempts to minimize the signal from the error microphone.

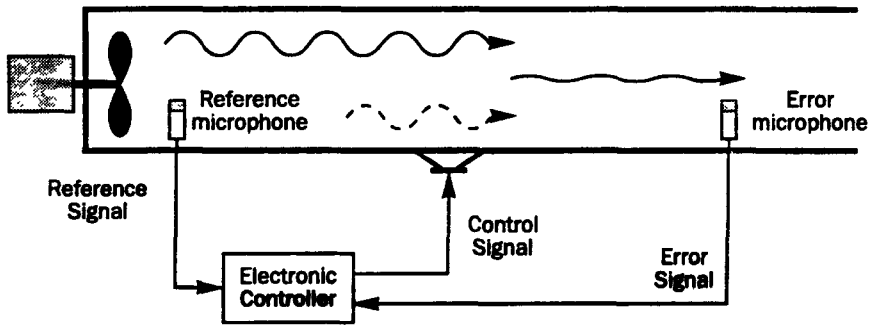

Figure 17 Basic active noise control system.

(b) Feedforward system

In Fig. 17b with feedforward control, the sound signal is sensed close to the source which is filtered by the electronic controller to produce the desired control signal fed to the actuator (a loudspeaker in this case). The controller attempts to minimize the signal measured by an error sensor (a microphone) using a control algorithm so that the error is minimized. Usually control is implemented digitally using a DSP chip, since in many cases analog circuitry is not practical. (An exception to this is the active hearing protector which normally uses analog control). In the active hearing protector the wavelength is always greater than the earcup cavity dimensions and the error sensor microphone and the noise control source can be collocated in the earcup. Since the passive noise protection of the earcup is normally adequate in the medium to high frequency range above about 1000 Hz, the active protection is only required in the low frequency range below that frequency. The feed back loop gain is normally maximized at about 200 Hz. [41] Figure 18 shows the noise attenuation of a typical commercial active hearing protector.

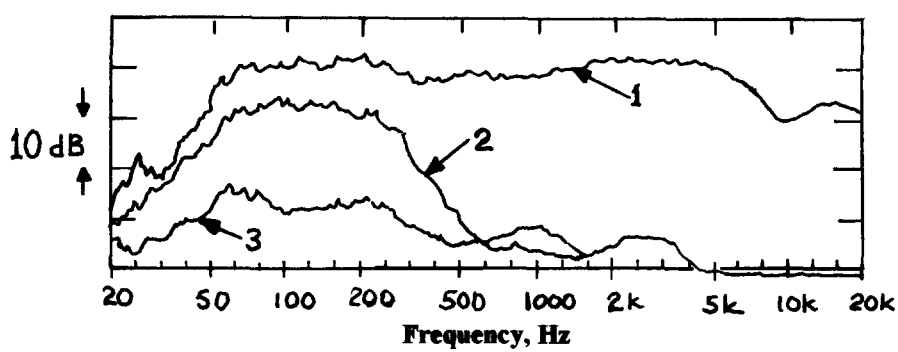

Figure 18. Attenuation provided by typical active hearing protector

1. Sound pressure level at ear of dummy head (no hearing protector)
2. Sound pressure level at ear of dummy head (with passive hearing protector)
3. Sound pressure level at ear of dummy head (with active hearing protector)

In the last three or four years considerable effort has been made to control the noise in the cabins of commercial aircraft using active noise control. The noise levels in many civilian turboprop aircraft and rotorcraft are uncomfortably high for the passengers and crew. They exceed the levels in comparable jet aircraft and thus these turboprop aircraft have received particular attention. The noise is dominated by the low frequency, pure tone, blade passing frequency (and multiples) of the propellers or rotor. This noise is transmitted through the cabin side walls to the cabin occupants. Active noise control is particularly attractive because pure tone noise is most easily controllable by this technology. Active noise control has been applied recently in the SAAB 2000, the SAAB 340plus and the ATR 42-500. [48,49] So far the approach has been to use feedforward control with loudspeakers in the cabin wall trim as the control actuators and error microphones in the cabin. The reference signals are obtained from synchronization signals taken from the propeller shafts. This approach has proved quite successful and cabin noise reductions of the order of 10 dB have been achieved. Figure 19a gives an example of the spectrum of the interior cabin noise. Figure 19b shows the average cabin sound pressure levels with different numbers of control loudspeakers in use. More recently another system has been used on the de Havilland DASH-8 aircraft range. [49] This system controls the cabin noise by active tuned vibration attenuators (ATVA's) which are attached to the fuselage frames in the region around the propeller plane. The ATVA's provide forces to the frames to oppose the fuselage deflections caused by the propeller excitation.
Another recent approach involves the reduction of cabin noise by control and minimization of the fuselage skin and/or the cabin trim vibration. [50-56] In such an approach the fuselage wall or cabin trim vibration is normally sensed with PVDF sensors and after processing such signals with a controller, these are fed back to PZT actuators. In some laboratory experiments reductions in the sound transmission through the walls and panels of over 10 dB have been achieved.

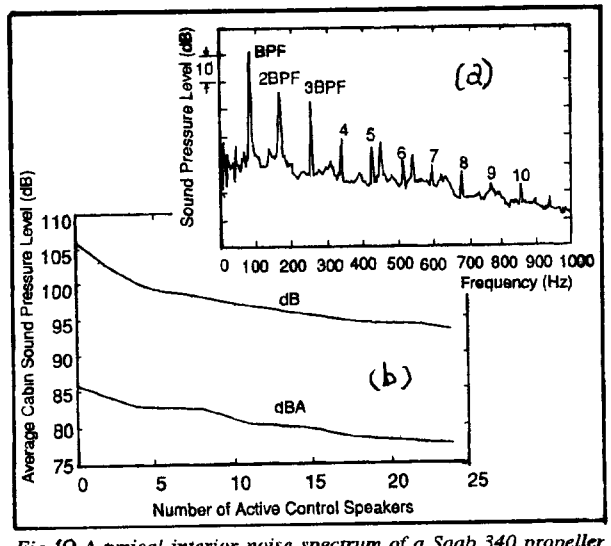

Fig.19 A typical interior noise spectrum of a Saab 340 propeller aircraft and average cabin sound levels with different numbers of active control speakers. The amount of achievable reduction increases with the number of speakers

Low frequency noise in heating, ventilating and air-conditioning (HVAC) ducts is a problem in many buildings. In many low frequency problems only the plane wave mode propagates making control relatively easy. The normal control approach is similar to that first proposed by Lueg [37] and consists of obtaining a reference signal from an upstream input microphone. This signal is fed through a controller consisting of an adaptive filter which removes the control feedback from the control signal into the reference sensor. The control signal is then fed to a loudspeaker positioned upstream of the input microphone. An error microphone is also located downstream and its signal is used to continuously update the controller via its stored algorithm. Figure 20 illustrates the performance of a commercial Digisonix sound cancellation system which achieved broadband noise reduction of the order of 11 to 13 dB when fitted to the supply duct of an industrial rooftop air handling system.

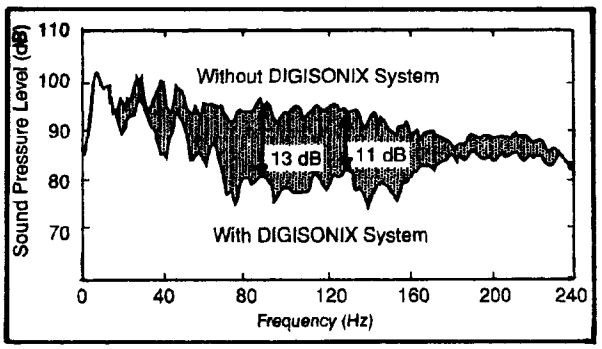

Fig. 20 Performance of a DIGISONIX Digital Sound Cancellation System retrofit to the supply duct of an industrial rooftop air handler. Broadband sound cancellation of 10 to 13 dB was achieved.

7.0 SOUND INTENSITY MEASUREMENTS

Sound intensity is a measure of the magnitude and direction of the flow of sound energy. Although Rayleigh attempted to measure sound intensity over 100 years ago and produced the well known Rayleigh disc that was used for many years, this was not a rugged device, and it is now thought that this measures the particle velocity squared. [57] Modern attempts to measure sound intensity resumed with Olsen's work in the 1930's [58], but were marred with experimental difficulties including phase shift errors. It was not until the late 1970's that the convergence of theoretical and experimental advances including the derivation of the cross spectral formulation for sound intensity and concurrent developments in digital signal processing propelled sound intensity measurements from the laboratory into practical use. [59,60] Sound intensity measurements seem to be most useful for the determination of the sound power of large machinery in situ, for noise source identification and for the transmission loss of partitions. [61,62] Care must be taken to sample the sound field appropriately in order to reduce errors. Calibration should be undertaken as recommended by the manufacturers and standards bodies. Crocker and Jacobsen have given a recent review of sound intensity measurements [63]. Fahy has written a recent book on the subject. [64]

Figure 21 shows how the sound power of a source can be measured. The sound power of the source is given by the integral of the product of the outgoing normal sound intensity I_n and the elemental control surface area dS over a measurement surface S enclosing the source. One great advantage of this approach to sound power determination is that sources *extraneous* to the control surface S do not affect the estimate of the sound power. This is because, provided that there is no sound absorbing material inside the control surface S , extraneous sound intensity that enters the surface also leaves it again and the errors cancel out. Since a perfect integration of $I_n\,dS$ over the surface S cannot be made in practice, either the integral is made by measuring I_n at a number of fixed points or obtaining the surface average of $I_n dS$ by moving the sound intensity probe at a steady speed (called *scanning*) over the measurement surface as illustrated in Fig 22.

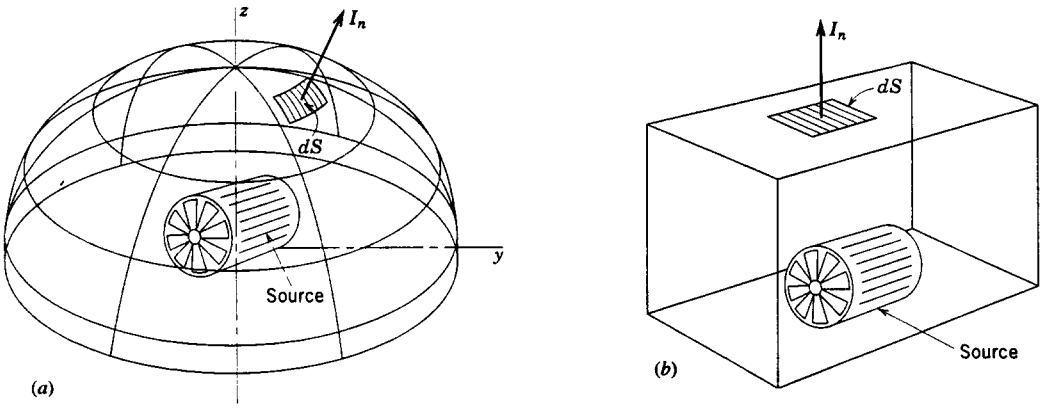

Fig. 21 Sound intensity measured on a segment of (*a*) a hemispherical measurement surface and (*b*) a rectangular measurement surface.

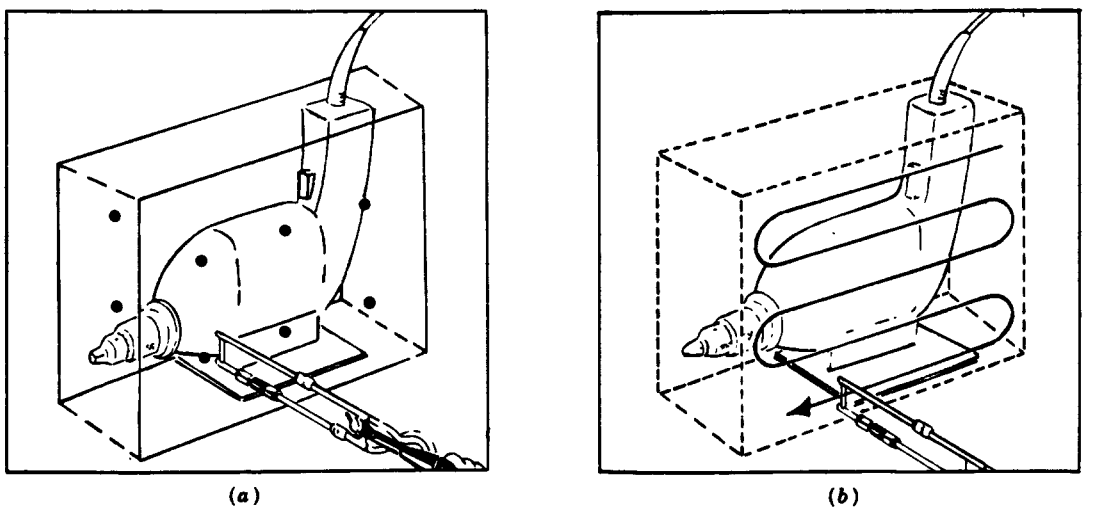

Fig. 22 Typical box surface used in sound power determina-tion with the intensity method: (*a*) measurements at discrete points and (*b*) measurement path used in scanning measurement. (After Rasmussen. ·)

Figure 23 shows the sound power of one part of a diesel engine obtained using the scanning approach. [65] The sound power of the oil pan (sump) of this engine was found to be the dominant noise source responsible for radiating half of the engine sound power. Vector plots of the sound intensity can also be useful in helping to identify the main noise sources in machinery as shown in Fig. 24. [66] The *transmission loss* (*sound reduction index*) of a partition can more easily be determined using sound intensity without the use of special facilities since a transmission suite is no longer needed (see Fig. 25) [67] and this approach also gives information about the transmission loss (TL) of individual parts of a composite panel such as the one in Fig. 26 which is made of aluminium with a Plexiglas (perspex) window. [68-71] The measurement of the sound power of sources using sound intensity measurements has been standardized by ISO, ANSI and other standards bodies and organizations. [72-74]. Instrumentation requirements for measuring sound intensity have also been standardized. [75,76] Efforts are underway to standardize the measurement of transmission loss using sound intensity. [77]

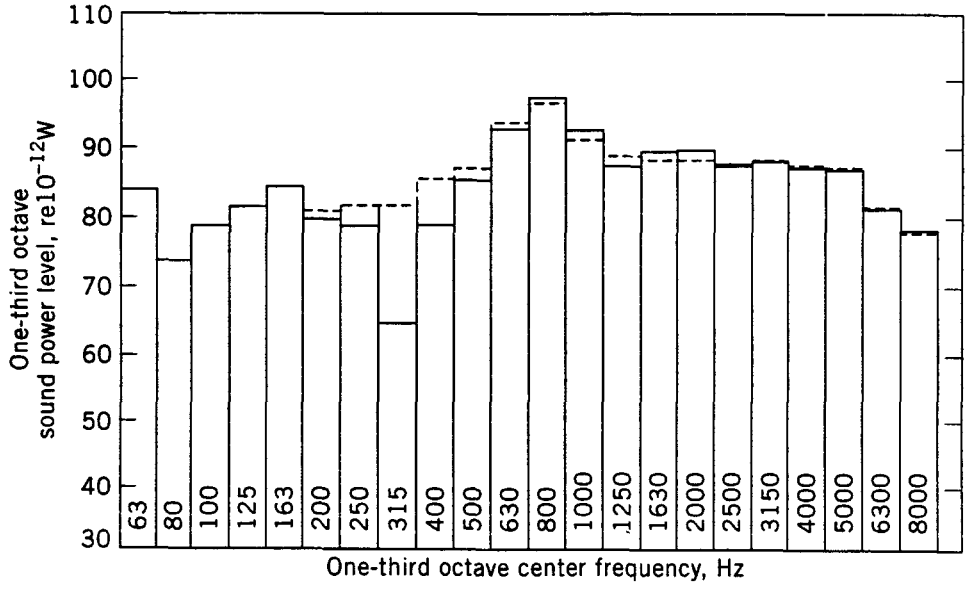

Fig. 23 The sound power of the oil pan of a diesel engine: ——, sound intensity method; ---, lead-wrapping results. (After Reinhart and Crocker.)

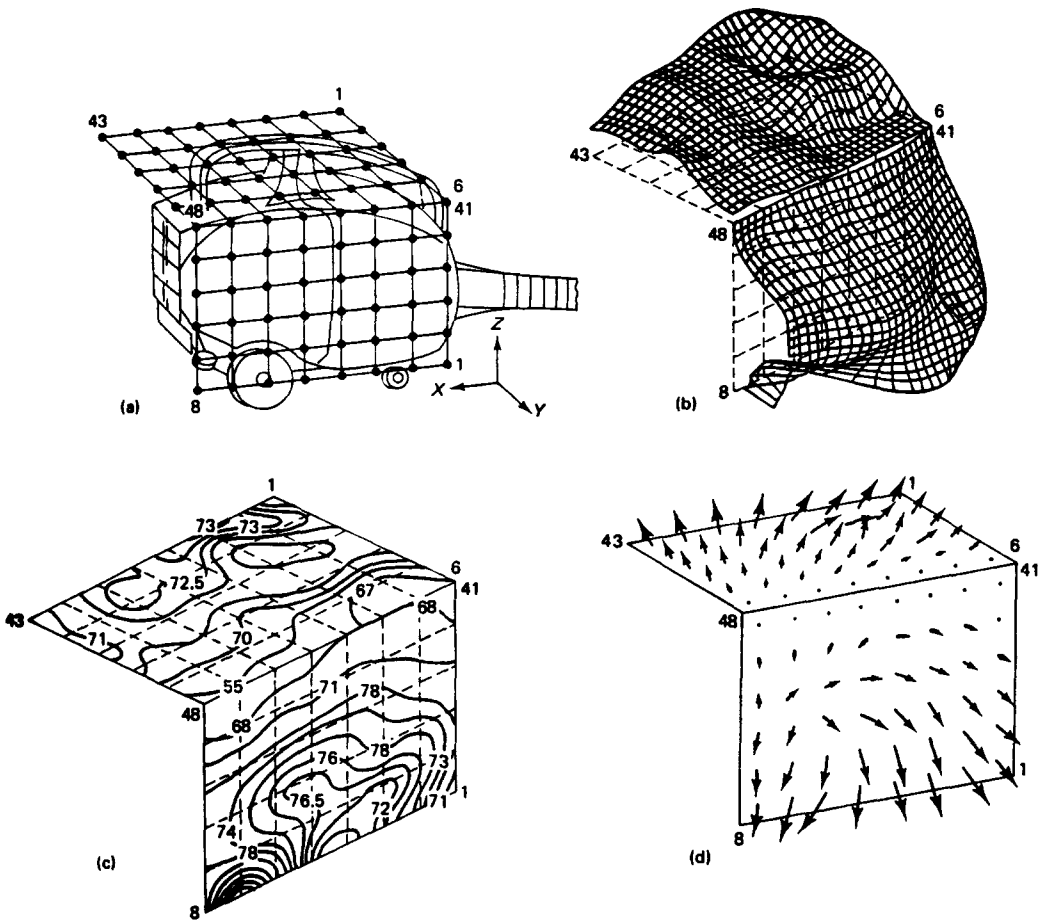

Fig. 24 Measurements of the sound intensity radiated by a vacuum cleaner: (*a*) vacuum cleaner and measurement points (two measurement surfaces each with 48 measurement points), (*b*) mesh diagram showing magnitude of normal intensity on the two surfaces, (*c*) contour plot showing contours of equal normal intensity on the two measurement surfaces, and (*d*) vector intensity flow diagram. (*Source:* RION Technical Notes.)

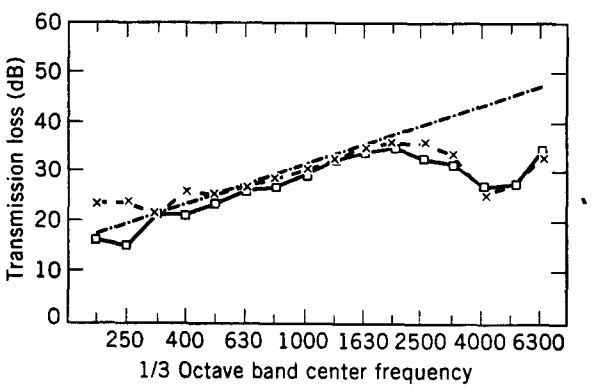

Fig. 25 Transmission loss of a 3.2 mm thick aluminum panel: □-□-□, Sound intensity method; × -- ×, conventional method; — · — · —, mass law. (After Crocker et al.)

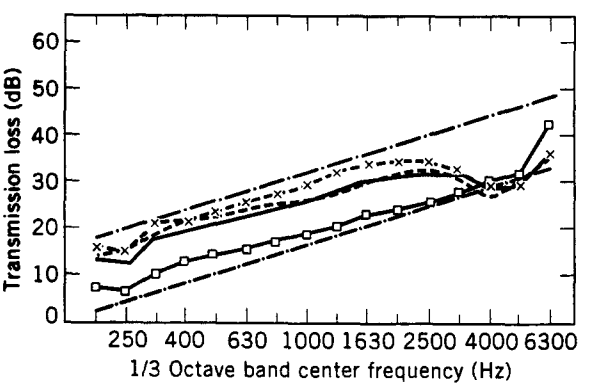

Fig. 26 Measured and calculated transmission loss of a composite aluminum-plexiglass panel. Measured values: × -- × -- ×, aluminum; □-□-□, plexiglass; - - -, total transmission loss. Calculated values; — · — · —, mass law, aluminum; – · – · – · –, mass law, plexiglass; ——— total transmission loss. (After Crocker et al.)

8.0 SPEECH SYNTHESIS AND RECOGNITION

The goal of designing a machine to recognize normal speech, understand it, and respond to it as a human does has not yet been fully achieved. However great strides have been made towards this goal in recent years. Flanagan has recently reviewed the field of speech synthesis and speech recognition. [78] Others have also reviewed these topics in recent years. [79-83]

8.1 Speech Synthesis.

In the ideal situation we should like a machine to synthesize the equivalent of spoken words from a printed text without any restriction on word vocabulary. This process is normally referred to as text-to-speech synthesis and is used in a number of financial systems in banks, insurance companies, etc. A system as in Figure 27 is commonly used. With the increased dictionary storage and computing power that recent rapid developments in digital computers have brought, improvements in speech synthesis have been apparent. The intelligibility of unrestricted text synthesis is quite good, but the speech presently often sounds artificial. Topics of current research include: 1) making the synthesis sound more natural, 2) synthesizing speech with a variety of accents and characteristics including personalizing the speech to represent individual voices, and 3) synthesizing speech in a variety of languages. [78]

8.2 Speech Recognition

Speech recognition is often used to provide access to machines or other systems via voice commands. The user normally speaks to (or commands) a machine. Currently there are three levels of speech recognition: 1) isolated word (or phrase) recognition in which the machine is taught or learns individual words (or phrases) and responds appropriately when these are spoken, 2) recognition of connected words where the machine learns a limited vocabulary of words and responds to a connected string of such spoken words from this vocabulary. (An example is a connected string of spoken digits in applications such as credit card validation, telephone dialing, menu-based access to information, etc.), and 3) continuous speech recognition in which the machine learns a vocabulary of basic speech units (or subwords) from which any spoken word can be created by using a sequence of subword units and use of a stored dictionary. This third level of speech recognition is often subdivided into: a) *transcription-like systems* (in which every word is recognized uniquely) and b) *spoken language understanding systems* (in which the speech, after recognition, is converted into a natural language question that need not correspond word-for-word with the recognized speech.) [78]

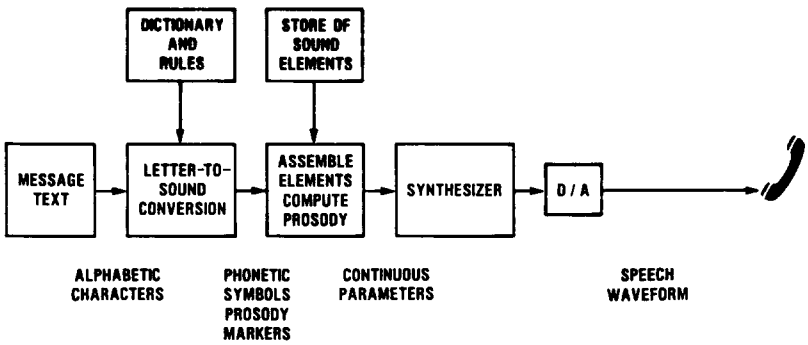

Fig. 27 Machine conversion of unrestricted printed text into natural-sounding speech requires transformation of the grapheme (alphabetic character) string into a phonetic equivalent, an understanding of the rules of language for the correct pronunciation of sounds and for voice inflection (pitch, intensity, and duration of successive sounds), and a means for controlling an electronic artificial vocal tract to yield an approximation to human speech.

The technology is now well established for very reliable recognition of individual words and phrases selected from vocabularies of large but limited size. An early successful procedure is to use a library of stored 'templates' for comparison with the words or phrases uttered. A vocabulary of templates containing the parameters describing the short time amplitude spectra of the allowed commands is stored digitally. An input command is measured and its spectrum is compared with the spectra of all of the stored vocabulary entries. (See Fig. 28). The comparison is normally made using an automatic time alignment procedure, known as a *dynamic time warp.* The closest fitting template in the library is chosen and the recognized word or phrase is normally repeated to the user using the machine's synthetic voice. The user is typically asked to confirm that the word or phrase has been correctly recognized. A more recent technique uses a statistical pattern recognition approach - called hidden Markov models (HMM's) - to estimate the sequence of words or speech sounds in continuous speech. A number of commercial vendors now offer automatic speech recognizers based on this principle. [67] Some speech recognition systems are designed to recognize speech and differentiate between the different individuals and recognize them. A system for talker verification is shown in Fig. 29. Recently some researchers have tried to coalesce the problems of speech coding, synthesis and recognition. One system designed to do this is shown in Fig. 30. [78]

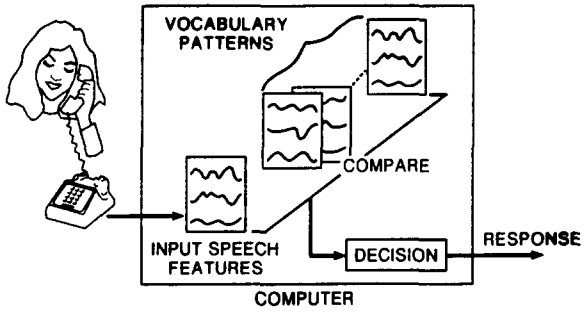

Fig. 28 Automatic speech recognition requires comparison of acoustic features measured for an unknown input with stored templates or statistical models for vocabulary items acceptable by the machine. The stored parameters describe short-time spectral characteristics of the vocabulary entries.

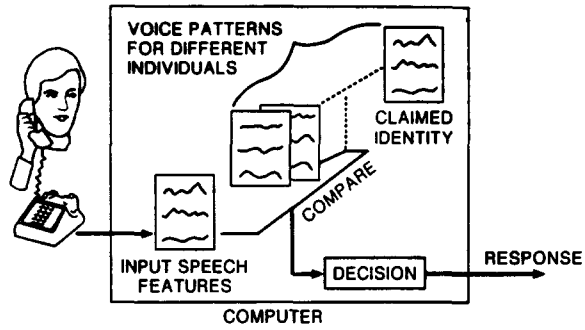

Fig. 29 Talker verification systems perform authentication of a claimed identity through measurements on the voice signal and comparison to a stored pattern known to characterize the claimed individual. A preassigned confidential code phase adds to the security. The machine measures the voice input, makes the comparison, and decides whether to accept or reject the identity claim.

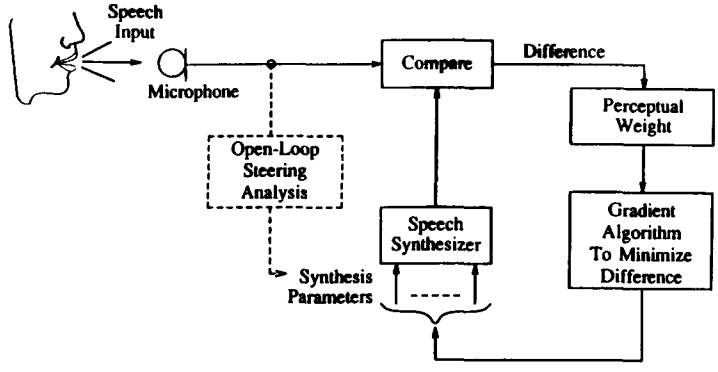

Possible Forms of Synthesis Parameters:
- Text
- Phonetic Symbols
- Articulatory Controls
- Spectrum-Describing Coefficients

Fig. 30 The voice mimic approach to speech processing aims to coalesce the problems of speech coding, synthesis, and recognition and achieve a contemporaneous solution through determination of compact signal-defining parameters.

9.0 ACOUSTICAL MEDICAL INSTRUMENTATION AND MEASUREMENTS

The use of ultrasound in medicine has had an increasing role in the last twenty years. It is used for several purposes including: 1) therapeutic heating, 2) surgical purposes, 3) passive analysis of heart and lung sounds for diagnosis, and 4) medical imaging. Greenleaf has written a recent review of acoustical medical instrumentation. [84] Shung and Cloutier have recently reviewed medical diagnosis using acoustics. [85] Bamber has recently discussed the properties of biological media that are important in obtaining information from medical ultrasound images. [86] These and other authors have also written extended monographs on these topics. [87,88]

Ultrasound is used for therapeutic heating, because unlike electromagnetic radiation, it combines a relatively great depth of penetration with a relatively short wavelength. It is thus possible to ensure that deep heating occurs in the localized tissues desired for treatment. The heat produced by the ultrasonic wave per unit volume is proportional to the negative divergence of the sound intensity in the wave. [84,85]

It has been known for a very long time that the sounds generated by the heart and lung carry useful information about the condition of these organs and can thus be used for medical diagnostics. [85] For many years the stethoscope has been used by physicians to facilitate better transmission of these sounds from the chest wall to the ear. However the stethoscope is hardly an ideal acoustic coupler or acoustic waveguide for transmission of sound over a broad frequency band. Recently Ultrasonic Doppler Flowmetry has been used to detect and analyze blood flow. [84,85]

For ultrasonic medical imaging and other related diagnostic applications, short wavelengths allow high resolution pictures of structures deep inside the body to be obtained. The use of ultrasonic medical imaging continues to grow because of the availability of real-time imaging, Doppler blood flow measurements, new transducer design, better signal processing, miniaturization and computerization of electronics, lack of x-ray radiation and exposure, and the high information/cost ratios of the images obtained. The medical fields of cardiology, obstetrics, gynecology, and other areas of medicine have been greatly impacted and advanced by the use of ultrasonic imaging technology. [84,85]

The transducer used must couple directly onto human tissue and must convert an electrical voltage pulse of several hundred volts into a sound pressure pulse in the tissue and then in a few microseconds receive the weak echoes that produce only a few microvolts of signal. Ceramic materials including lead zirconate-titanate, modified lead titanate and lead metaniobate are the most commonly used transducer materials. Transducers made from disks or arrays of solid-phase ceramics are used but have the disadvantage that their impedance (of the order of 20-30 Mrayl) is too high to match efficiently to tissues even with matching layers. [84] Transducers made from composites or piezocomposites are to be preferred since their lower impedance of about 6 Mrayl more closely matches that of human tissue. Such transducers are

made by kerfing the solid-phase material rods (often PZT) and backfilling the kerfs with a polymer matrix such as PVDF to obtain the better transducer properties desired and provide better impedance matching with the tissue. (See Fig. 31) [84] Different transducer geometries are possible but the principal ones are rectangular (linear arrays) and circular. A typical ultrasonic medical imaging system is shown in Fig 32. [84] The transducer transmits a short pulse of ultrasonic waves into the tissue. Then it receives reflected waves that are in turn converted into an electrical signal. An ultrasonic beam is formed in both the transmission and reception phases of the process. The beam forming is done either 1) physically with lenses or curved transducer elements or 2) electronically. Electronic beam forming in the transmission phase is carried out by sending phased pulses from the elements of the transducer array to produce a beam focused at some chosen depth. In the reception phase, the echo signal pattern desired is formed by individually amplifying, delaying and then summing the signals received by the transducer elements. The reflected signals thus received are processed to produce images of the scattering tissue or alternatively to obtain Doppler frequency shifts that indicate blood flow. The flow speed, tissue attenuation and other tissue properties must be properly accounted for. The processed information is then displayed in some logical, consistent way for the user. The echo amplitude distribution is mapped onto the viewing system. Provision is normally made for the recording of static and dynamic images from the screen and for their storage and subsequent retrieval.

The reflected or scattered sound waves can also be used to detect the fluid motion through the Doppler effect. Doppler shift instrumentation uses either continuous wave or pulsed signals. The signals scattered by the blood cells are processed either in the frequency or the time domain. The relative direction of the beam and of the blood flow must be known if a quantitative knowledge of the flow velocity is desired. Doppler information can be included in B-scan images using colour. The usual convention is to use blue colours to show the flow

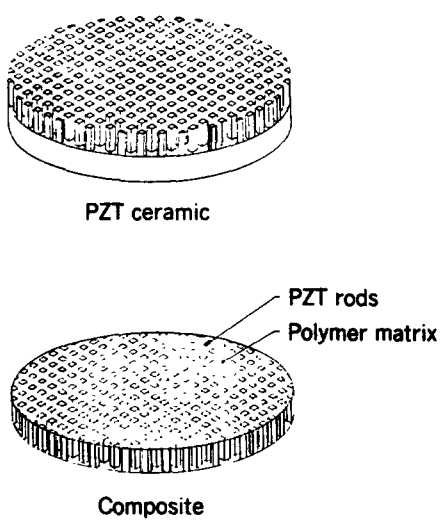

Fig. 31 Composite transducers are made from solid-phase transducers by dicing with a saw and backfilling the kerfs with a polymer. The resulting transducer has low impedance and high coupling constant in addition to physical flexibility. (Reproduced, with permission, from W. A. Smith and A. A. Shaulov, "Composite Piezo electrics: Basic Research to a Practical Device," *Ferroelectrics*, Preprint, 1988, pp. 1–12.)

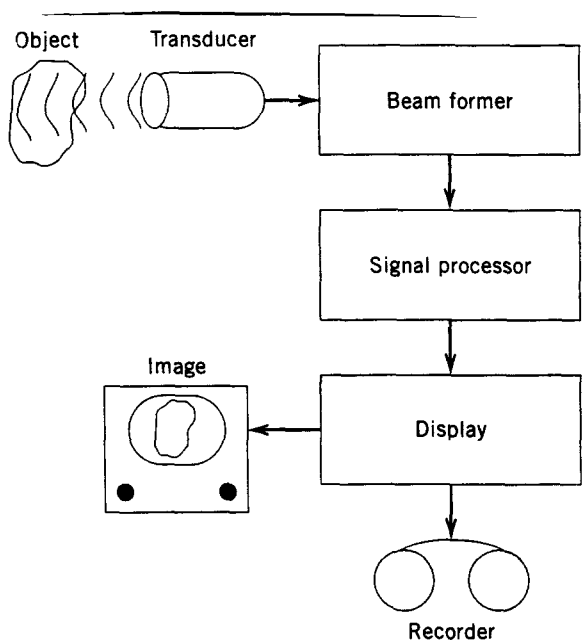

Fig. 32 Principal components of the imaging system are the transducer, the beamformer, the signal processor, the display, and the recorder.

velocity away from the ultrasonic probe and red to show the flow velocity towards the probe. With some systems the user can switch the colours to correspond to arterial and venous flow. Turbulence is normally shown in green and the stronger the turbulence the greener the colour. Fig. 33 shows an image of a carotid artery. This image was obtained by placing the transducer on the neck of the subject above the carotid artery. [84] Fig 34 shows an image of the heart showing an atrial septal defect. The image was obtained by placing an ultrasound array on the end of an endoscope located in the esophagus. The images are reconstructed into a three-dimensional image in Fig 35.

Fig. 33 Image of a carotid artery. As a color distribution in a B-scan image, the lower flow would be colored red for a Doppler-detected flow toward the transducer in the carotid artery, and the upper flow would be colored blue for flow away from the transducer in the jugular vein.

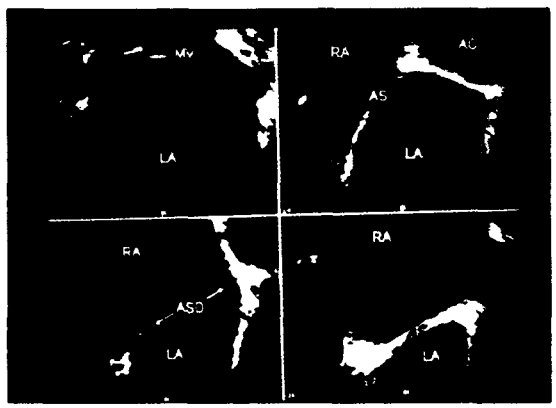

Fig. 34 Atrial septal defect imaged by transesophageal probe placed within the esophagus near the base of the heart. (Examples from series of 50 consecutive slices.) (AO, aorta; AS, atrial septum; LA, left atrium; MV, mitral valve; RA, right atrium; viewpoint of three-dimensional reconstruction shown in Fig. 35)

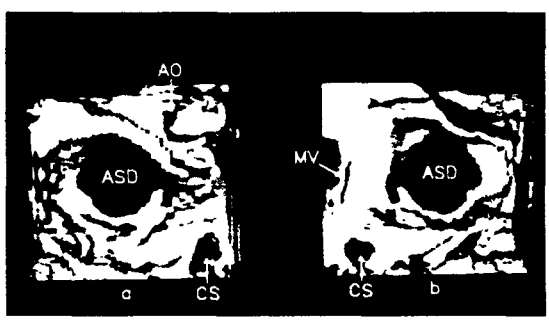

Fig. 35 Transesophageal probe was rotated to obtain scattering from a three-dimensional volume containing the base of the heart. The resulting set of images were used to reconstruct this image of the atrial septum and its defect. View from (a) the right atrium and (b) the left atrium (AO, aortic valve; CS, coronary sinus; MV, mitral valve).

Fig 36 shows a region of the colon with cancer. The cancerous region is the dark area. The image was obtained with a transrectal probe. Rectal probes can also be used to obtain images of the prostate. Fig 37 was obtained with a transvaginal probe. It shows an intrauterine pregnancy. The ovaries can also be imaged using this probe. Finally Fig. 38 shows an intravascular image of a coronary artery containing some atheroscelerotic plaque. [84]

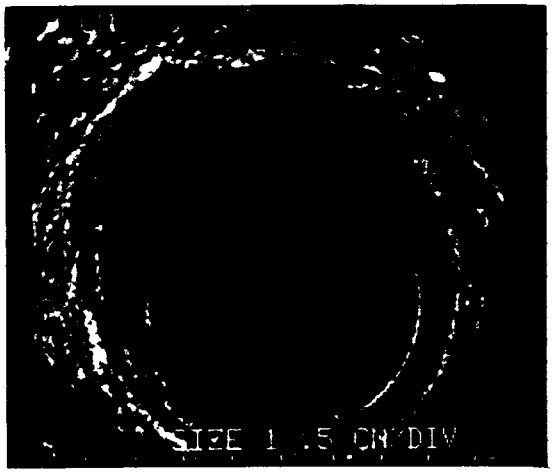

Fig. 36 Image of colon cancer (dark region) obtained from a transrectal ultrasonic probe.

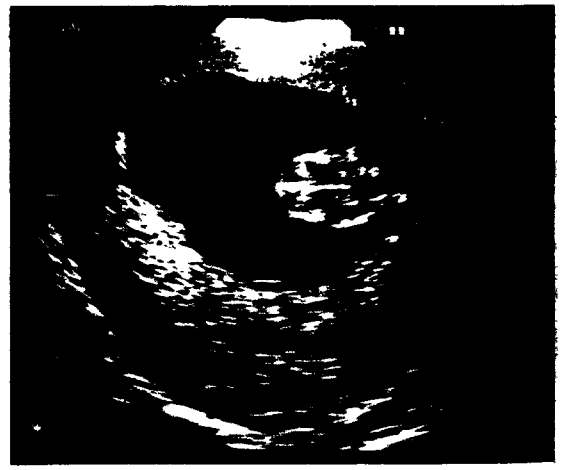

Fig. 37 Intrauterine pregnancy imaged by a transvaginal probe.

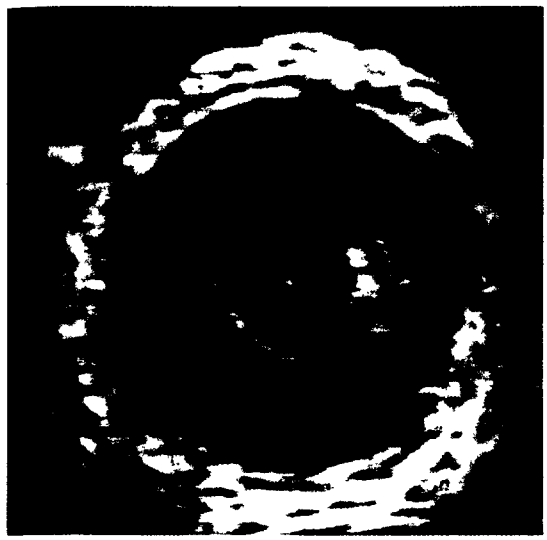

Fig. 38 Intravascular image obtained with an array at the tip of catheter in a coronary artery.

10.0 HEARING AND THE COCHLEA

During the 1970's and 1980's extensive knowledge has been gained into the understanding of the hearing sensitivity of man and other mammals [89]. This was made possible by several new measurement techniques including the implementation of Mossbauer sources. [90,91] This allowed the *in vivo* determination of the tuning curves for basilar-membrane vibrations, near the base of the cochlea, for sound levels of over 70 dB. These results revealed that the cochlea possesses very much greater tuning capabilities than earlier measurements (made on cadavers) had suggested. [92]

Further measurements for sound levels of 20 dB or less (made after this technique was refined further) have indicated an even further enormous increase in the sharpness of tuning. This suggests that the sharpness of tuning for the basilar membrane vibrations is similar to the very sharp tuning of the auditory nerve fibres. In the late 1970's Kemp discovered the existence of evoked otoacoustic emissions. [93] As described by Lighthill [94] the analysis of these data suggest that the cochlea performs its well known frequency analysis and obtains its sensitivity to sound at low levels from two main mechanisms. These are:

1) its passive frequency response which occurs because of the steeply graded stiffness variation in the basilar membrane which is immersed in the cochlear fluids. Sound signals at different frequencies become separated from each other with each frequency component completing its passage at its characteristic location on the cochlear at which the local *inner* hair cells generate stimuli that are sent along particular auditory nerve fibres to the cortex.

2) at very low sound levels it has recently been found that there is an active frequency response system related to the *outer* hair cells. These, through a process of positive feedback, amplify the vibrations of the basilar membrane in a healthy cochlea. This process produces an enhanced signal at low sound levels, so that the threshold at which they can generate activity in the auditory nerve fibres is very much lowered. The *outer* hair cells posses the ability to go into continuous vibration at a particular sound frequency which is sustained by a metabolic power source. Since these vibrations can be stimulated by a very small sound signal they can (on their communication to the basilar membrane) produce a significant enhanced stimulus to the *inner* hair cells.

Figure 39 shows a drawing of the cortical lattice in tangential and transverse section. Figure 40 shows a diagram of the location of the lattice in the cortex of an outer hair cell. Figure 41 shows a possible molecular basis for the outer hair cell motor. [94] The area change in the molecule is transformed into a change in cell length. [94]. The functioning of the outer hair cells has been recently described by Ashmore and others in a series of papers. [95-105]

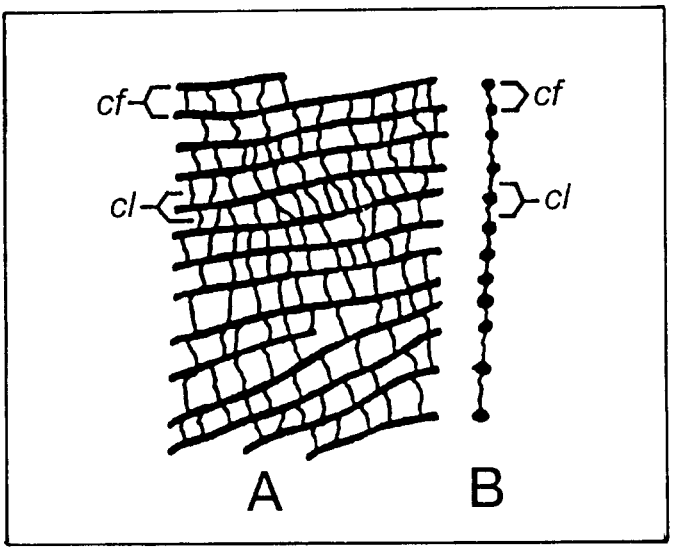

Figure 39 Drawing of the extracted cortical lattice in tangential (A) and transverse (B) section. Note the absence of pillars that are available in Fig. 40 *cf*, circumferential filaments; *cl*, cross-links.

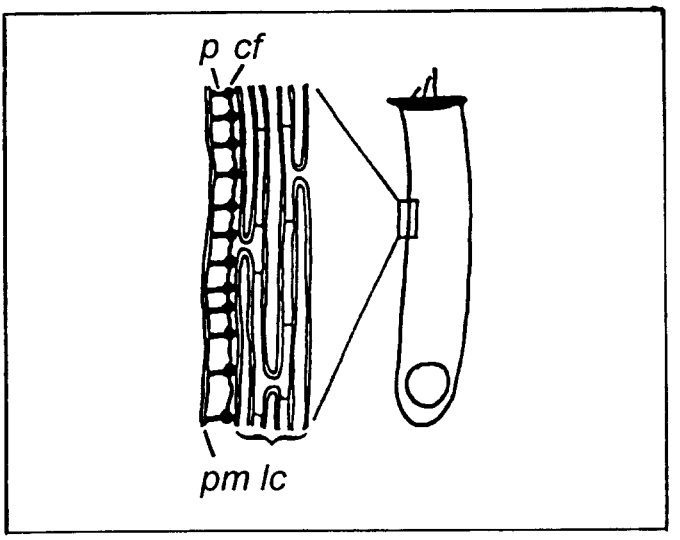

Figure 40 Diagram illustrating the location of the lattice in the cortex of an outer hair cell. *pm*, plasma membrane; *lc*, lateral cisternae; *p*, pillars; *cf*, circumferential filaments.

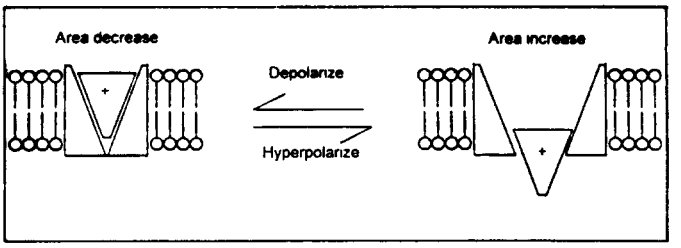

Figure 41 A possible molecular basis for the outer hair cell motor. The molecule is regarded as capable of undergoing a conformation change and, as it does so, a charge is transferred across the membrane. Measurement of the total charge transferred gives an estimate of the number of such 'particles' present in the membrane. The area change in the molecule is transformed as a change in cell length.

ACKNOWLEDGMENTS

The help of the following colleagues who kindly provided assistance in the way of useful comments, figures for the text and in some cases slides for the verbal presentation is gratefully acknowledged: Anthony Craggs, James L. Flanagan, Christopher R. Fuller, James F. Greenleaf, Colin H. Hansen, Geoffrey Lilley, Sir James Lighthill, Phillip A. Nelson, Andrew F. Seybert, K. Kirk Shung, Norma B. Slepecky, Gregory W. Swift, Several parts of this review paper are drawn in part from material authored by some of the colleagues above in the Encyclopedia of Acoustics (M. J. Crocker, Editor) John Wiley and Sons, New York, 1997.

REFERENCES

1. M. Petyt, Introduction to Finite Element Analysis, Cambridge University Press, Cambridge, 1990.

2. A. Craggs, Acoustic Modeling: Finite Element Method, Chapter 14 in Encyclopedia of Acoustics, M. J. Crocker (Ed), John Wiley & Sons, New York, 1997.

3. A. Craggs, The Use of Simple Three Dimensional Acoustic Finite Elements for Determining the Natural Modes and Frequencies of Complex Shaped Enclosures, *J. Sound and Vibration* , Vol. 23, pp. 331-339, 1972.

4. C .I .J. Young and M. J. Crocker, Finite Element Acoustical Analysis of Complex Muffler Systems with and without Wall Vibrations, *Noise Control Engineering Journal,* Vol. 9, No. 2, pp. 86-93, 1977.

5. C. I. J. Young and M. J. Crocker, Prediction of Transmission Loss in Mufflers by the Finite Element Method, *J. Acoust. Soc. Amer., Vol. 57,* pp. 144-148, 1975.

6. C. I. J. Young and M. J. Crocker, Acoustical Analysis Testing and Design of Flow-Reversing Muffler Chambers, *J. Acoust. Soc. Amer.*, Vol. 60, pp. 1111-1118, 1976.

7. A. F. Seybert and T. W. Wu, Acoustic Modeling: Boundary Element Methods, Chapter 15 in Encyclopedia of Acoustics, M. J. Crocker (Ed), John Wiley & Sons, New York, 1997

8. M. A. Hamadi, Recent Advances in Vibro-Acoustic Computation, *Noise-Con 97*, Penn State, PA, 1997.

9. G. M. Lilley, X. Zhang and A. Rona, Progress in Computational Aeroacoustics in Predicting the Noise Radiated from Turbulent Flows, *International Journal of Acoustics and Vibration*, Vol. 2, No. 1, pp. 3-10, 1977.

10. S. Lee and W.C. Meecham, Computation of Noise and Homogeneous Turbulence from a Free Jet, *International Journal of Acoustics and Vibration,* Vol. 1, No. 1, pp. 35-47, 1996.

11 S. C. Borgowda, U. S. Shirahatti, A. Klotchov and M. J. Crocker, Computational Aeroacoustic Analysis of Ducts, *Proc. Third International Congress on Air- and Structure-borne Sound and Vibration,* Montreal, Canada, pp. 1265-1268, 1994.

12. P. Morris, Analytical and Numerical Predictions of High Speed Jet Noise, Paper AIAA-97-1598, *Third AIAA/CEASA Aeronautics Conference*, Atlanta, May 1997.

13. C. K. W. Tam, Computation of Mean Flow Refraction Effects on Jet Noise, Paper AIAA-97-1599, *Third AIAA/CEASA Aeronautics Conference,* Atlanta, May 1997.

14. X. Zhang and J. A. Edwards, An Investigation of Supersonic Oscillatory Cavity Flow Driven by a Thick Shear Layer, *The Aeronautical Journal*, Vol. 94, pp. 355-364, 1990.

15. X. Zhang, A. Rona and G. M. Lilley, Far Field Noise Radiated from Unsteady Supersonic Cavity Flow, *Proceedings CEAS/AIAA Aeroacoustics Conference, Munich, Germany,* 1995.

16. K. S. Suslick and L. E. Crum, Sonochemistry and Sonoluminescence, Chapter 26 in Encyclopedia of Acoustics, M. J. Crocker (Ed), John Wiley & Sons, New York, 1997.
17. K. S. Suslick, Applications of Ultrasound to Materials Chemistry, *MRS Bulletin*, Vol. XX, No. 4, 1995.
18. K. S. Suslick, The Temperature of Cavitation, Science, Vol. 253, pp. 1397-1399, 1991.
19. K. S. Suslick (Ed), Ultrasound: Its Chemical , Physical and Biological Effects, VCH Publishers, New York, 1988.
20. T. J. Mason (Ed), Advances in Sonochemistry, Vols. 1-3, JAI Press, New York, 1990, 1991, 1993.
21. T. J. Mason and J. P. Lorimer, Theory, Applications and Uses of Ultrasound in Chemistry, Ellis Horwood, Chichester, United Kingdom, 1988.
22. G. J. Price (Ed), Current Trends in Sonochemistry, Royal Society of Chemistry, Cambridge, 1992.
23. O. V. Abramov, Ultrasound in Liquid and Solid Metals, CRC Press, Boca Raton, FL, 1994.
24. T. G. Leighton, The Acoustic Bubble, Academic Press, London, pp. 531-551, 1994.
25. G. W. Swift, Thermoacoustic Engines, Chapter 61 in Encyclopedia of Acoustics, M. J. Crocker (Ed), John Wiley & Sons, New York , 1997.
26. G. W. Swift, Thermoacoustic Engines and Refrigerators, *Physics Today*, pp. 22-28, July 1995.
27. G. W. Swift, Thermoacoustic Engines, *J. Acoust. Soc. Amer.*, Vol. 84, pp. 1145-1180, 1988.
28. W. P. Arnott, H. E. Bass and R. Raspet, General Formulation of Thermoacoustics for Stacks Having Arbitrarily Shaped Pore Cross Sections, *J. Acoust. Soc. Amer.*, Vol. 90, p 3228-3237, 1991.
29. G. W. Swift and R. M. Keolian, Thermoacoustics in Pin-Array Stacks, *J. Acoust. Soc. Amer.*, Vol. 94, pp. 941-943, 1993.
30. W. C. Ward and G. W. Swift, Design Environment for Low Amplitude Thermoacoustic Engines, *J. Acoust. Soc. Amer.*, Vol. 95, pp. 3671-3672, 1994
31. J. R. Olson and G. W. Swift, Similitude in Thermoacoustics, *J. Acoust. Soc. Amer.*, Vol. 95, pp. 1405-1412, 1994.
32. R. Radebaugh., A Review of Pulse Tube Refrigeration, *Adv. Cryogenic Eng.*, Vol. 35, pp. 1191-1205, 1990.
33. S. Zhu, P. Wu and Z. Chen, Double Inlet Pulse Tube Refrigerators: An Important Development, *Cryogenics*, Vol. 30, p. 514, 1990.
34. Lord Rayleigh (J. W. Strutt), The Theory of Sound, Second Edition, Cambridge University Press, Cambridge, Sect. 322, 1894-5.
35. T. Hofler, Concepts for Thermoacoustic Refrigeration and a Practical Device, in *Proc. 5th Int Cryocoolers Conf., Monterey, CA,* p.93, August 1988.
36. G. W. Swift, Thermoacoustic Natural Gas Liquifier, *DOE Natural Gas Conference, Houston, TX,* pp. 1-4, March 1997.
37. P. Lueg, Process of Silencing Sound Oscillations, U.S. Patent No. 2,043,416, 1936.
38. P. A. Nelson and S. J. Elliott, Active Noise Control, Chapter 84 in Encyclopedia of Acoustics, M. J. Crocker (Ed), John Wiley & Sons, New York, 1997.
39. C. R. Fuller, Active Vibration Control, Chapter 75 in Encyclopedia of Acoustics, M. J. Crocker (Ed), John Wiley & Sons, New York, 1997.
40. C. H. Hansen, Active Noise Control - From Laboratory to Industrial Implementation, *Noise-Con 97 Procs., University Park, PA, Book* 2, pp. 3-38, 1997.

41. C. R. Fuller and A. H. von Flotow, Active Control of Sound and Vibration, *IEEE Control Systems,* December, 1995, pp. 9-19.

42. E. F. Crawley, Intelligent Structures for Aerospace: A Technology Overview and Assessment, *AIAA Journal*, pp. 1689-1699, August 1994.

43. P. A. Nelson and S. J. Elliott, Active Control of Sound, Academic Press, London, 1992.

44. M. O. Tokhi and R. R. Leitch, Active Noise Control, Oxford University Press, 1992.

45. S. M. Kuo and D. R. Morgan, Active Noise Control Systems, John Wiley & Sons, New York, 1996.

46. C. R. Fuller, S. J. Elliott and P. A. Nelson, Active Control of Vibration, Academic Press, London, 1996.

47. C. H. Hansen and S. D. Snyder, Active Control of Noise and Vibration, E&FN Spon, London, 1997.

48 U. Emberg, Application of Active Noise Control in Saab 340 and Saab 2000, *Proceedings of the Nordic Conference on Vehicle and Machinery Vibrations,* Stockholm, September 1994.

49. C. F. Ross and M. R. J. Purver, Active Cabin Noise Control, *Active 97 Proceedings,* Budapest, Hungary, pp. xxxix-xlvi, 1997.

50. M. J. Crocker, X. C. Yan, W. Kowbel and V. Chellappa, Feedback Control of Vibration of a Rectangular Panel to Increase its Transmission Loss, *Proceedings of the Fourth International Congress on Sound and Vibration,* St. Petersburg, Russia, 1996.

51. D. R. Thomas, P. A. Nelson, S. J. Elliott and R. J. Pinnington, An Experimental Investigation into the Active Control of Sound Transmission through Stiff Light Composite Panels, *Noise Control Engineering Journal,* Vol. 41, Num. 1, pp. 145-154, 1993.

52. M. Viscardo and L. Lecce, Experiences of Active Vibration Control on Typical Aeronautical Structures, *Active 97 Proceedings*, Budapest, Hungary, pp. 145-154, 1997.

53. B. N. Tran and G. P. Mathur, Aircraft Interior Noise reduction Tests using Active Trim Panels, *Procs. of Noise-Con 96*, Seattle, Washington, pp. 395-400, 1996.

54. R. J. Silcox, C. R. Fuller and R. A. Burdisso, Concepts on an Integrated Design Approach to the Active Control of Structurally Radiated Noise (ASAC), *Transactions of ASME*, Vol. 117, pp. 261-270, 1995

55. D. G. MacMartin, Collocated Structural Control for the Reduction of Aircraft Cabin Noise, *Journal of Sound and Vibration,* Vol. 190, Num. 1, pp. 105-119, 1996.

56. K. H. Lyle and R. J. Silcox, Active Trim Panels for Aircraft Interior Noise Reduction, *Aerospace Engineering*, Warrendale, PA, Vol. 15, Num. 12, pp. 21-25, 1995.

57. M. J. Crocker, Direct Measurement of Sound Intensity and Practical Applications In Noise Control Engineering, *Inter-Noise 84 Proceedings*, pp. 19-36, 1984.

58. H. F. Olson, System Response to the Energy Flow of Sound Waves, U.S. Patent No. 1,892,644, 1932.

59. F. J. Fahy, Measurement of Acoustic Intensity Using the Cross-Spectral Density of Two Microphone Signals, *J. Acoust. Soc. Amer.* Vol. 62, pp. 1057-1059, 1977.

60. J-Y Chung, Cross Spectral Method of Measuring Acoustic Intensity without Error Caused by Instrumentation Phase Mismatch, *J. Acoust. Soc. Amer.* Vol. 64, pp. 1613-1616, 1978.

61. W. P. Waser and M. J. Crocker, Introduction to the Two-Microphone Cross Spectral Method of Determining Sound Intensity, *Noise Control Engineering Journal,* Vol. 22, pp. 76-85, 1984.

62. M. J. Crocker, Sound Intensity, Chapter 14 in Handbook of Acoustical measurements and Noise Control, C. M. Harris (Ed), Third Ed., 1991.

63. M. J. Crocker and F. Jacobsen, Sound Intensity, Chapter 156 in Encyclopedia of Acoustics, M. J. Crocker (Ed), John Wiley & Sons, New York, 1997.
64. F. J. Fahy, Sound Intensity, Second Edition, E&FN Spon, London, 1995
65. T. E. Reinhart and M. J. Crocker, Source Identification on a Diesel Engine Using Acoustic Intensity Measurements , *Noise Control Engineering Journal,* Vol. 18, pp. 84-92, 1982
66. Rion Technical Notes.
67. M. J. Crocker, P. K. Raju and B. Forssen, Measurement of Transmission Loss of Panels by the Direct Determination of Transmitted Acoustic Intensity, *Noise Control Engineering Journal,* Vol. 17, pp. 6-11, 1981.
68. Y. S. Wang and M. J. Crocker, Direct Measurement of Transmission Loss of Aircraft Structures Using the Acoustic Intensity Approach, *Noise Control Engineering Journal,* Vol. 19, pp. 80-85, 1982.
69. Y. S. Wang, M. J. Crocker and P. K. Raju, Theoretical and Experimental Evaluation of Transmission Loss of Cylinders, *AIAA Paper 81,* 1981 and *AIAA Journal,* Vol. 21, No. 3, pp. 186-192, 1983.
70. K. H. Lyle, M. S. Atwal, M. J. Crocker, Light Aircraft Sound Transmission Studies: The Use of the Two-Microphone Sound Intensity Technique, *Noise Control Engineering Journal,* Vol. 31, No. 3, pp. 145-151, 1988.
71. M. S. Atwal, K. E. Heitman, and M. J. Crocker, Light Aircraft Sound Transmission Studies: Noise Reduction Model, *J. Acoustical Soc. of America,* Vol. 82, No. 4, pp. 1342-1348, 1987.
72. ANSI S12.12-1992, Engineering Method for the Determination of Sound Power Levels of Noise Sources Using Sound Intensity, 1992.
73. ISO 9614-1, Acoustics-- Determination of Sound Power Levels of Noise Sources Using Sound Intensity -- Part 1: Measurement at Discrete Points, 1993.
74. ISO 9614-2, Acoustics-- Determination of Sound Power Levels of Noise Sources Using Sound Intensity -- Part 2: Measurement by Scanning, 1996.
75. IEC 1043, Instruments for the Measurement of Sound Intensity, 1993.
76. ANSI S1-12-1994, Instruments for the Measurement of Sound Intensity, 1994.
77. DIS 140. Acoustics -- Measurement of Sound Insulation in Buildings and of Building Elements -- Part 5: Field Measurements of Airborne Sound Insulation of Facade Elements and Facades.
78. J. L. Flanagan, Introduction (to Speech Recognition), Chapter 124, Encyclopedia of Acoustics, M. J. Crocker (Ed), John Wiley & Sons, New York, 1997.
79. S. Furui, Digital Speech Processing, Synthesis and Recognition, Marcel Dekker, New York, 1989.
80. D. O'Shaughnessy, Speech Communication: Human and Machine, Addison Wesley, New York, 1987.
81. N. S. Jayant and P. Noll, Digital Coding of Waveforms, Prentice Hall, Engelwood Cliffs, NJ, 1984.
82. E. A. Lee and D. G. Messerschmitt, Digital Communication, Kluwer, Boston, 1988.
83. T. Parsons, Voice and Speech Processing, McGraw-Hill, New York, 1987.
84. J. F. Greenleaf, Acoustical Medical Imaging Instrumentation, Chapter 144 in Encyclopedia of Acoustics, M. J. Crocker (Ed), John Wiley & Sons, New York, 1997.
85. K. S. Shung and G. Cloutier, Medical Diagnosis with Acoustics, Chapter 143 in Encyclopedia of Acoustics, M. J. Crocker (Ed), John Wiley & Sons, New York, 1997.
86. J. C. Bamber, Acoustical Characteristics of Biological Media, Chapter 141 in Encyclopedia of Acoustics, M. J. Crocker (Ed), John Wiley & Sons, New York, 1997.

87. J. F. Greenleaf, Tissue Characterization with Ultrasound, Vols. I and II, CRC Press, Boca Raton, FL, 1986.

88. K. K. Shung and G. A. Thieme, Ultrasonic Scattering in Biological Tissues, CRC Press, Boca Raton, FL, 1993.

89. J. Lighthill, Biomechanics of Hearing Sensitivity, *ASME Journal of Vib. Acoust.* Vol. 113, pp. 1-13, 1991.

90. B. M. Johnstone, K. J. Taylor and A. J. Boyle, Mechanics of the Guinea Pig Cochlea, *Journal of Acoust. Soc. Amer.*, Vol. 47, pp. 504-509, 1970.

91. W. S. Rhode, Observations of the Vibration of the Bassilar Membrane in Squirrel Monkeys Using the Mossbauer Technique, *Journal of Acoust. Soc. Amer.*, Vol. 49, pp. 1218-1231, 1971.

92. G. Von Bekesy, Experiments in Hearing, McGraw-Hill, New York, 1960.

93. D. T. Kemp, Stimulated Acoustic Emissions from the Human Auditory System, *Journal of Acoust. Soc. Amer.*, Vol. 64, pp. 1386-1391, 1978.

94. J. Lighthill, Recent Advances in Interpreting Hearing Sensitivity, *International Journal of Acoustics and Vibration*, Vol. 1, No. 1, pp. 5-9, 1996.

95. A. J. Hudspeth, The Cellular Basis of Hearing, *Science*, Vol. 230, pp. 745-752, 1985.

96. M. C. Holley and J. F. Ashmore, On the Mechanism of a High Frequency Force Generator in Outer Hair Cells Isolated from the Guinea Pig Cochlea, *Proc. Roy Soc. B*, Vol. 232, pp. 413-429, 1988.

97. J. F. Ashmore, The Cellular Machinery of the Cochlea, *Exper. Physiol.*, Vol. 79, pp. 113-134, 1994.

98. M. C. Holley and J. F. Ashmore, On the Mechanism of a High-frequency Force Generator in Outer Hair Cells Isolated From the Guinea Pig Cochlea, Proc. Roy. Soc., B232, pp. 413-429, 1988.

99. M. C. Holley and J. F. Ashmore, A Cytoskeletal Spring in Cochlear Outer Hair Cells, *Nature*, Vol. 335, pp. 635-637, 1988.

100. M. C. Holley and J. F. Ashmore, Spectrin, Actin and the Structure of the Cortical Lattice in Mammalian Outer Hair Cells, *Journal Cell. Sci*, Vol. 96, pp. 283-291, 1990.

101. J. F. Ashmore, Transducer-Motor Coupling in Cochlear Outer Hair Cells, *Cochlear Mechanisms- Structure, Function and Models*, pp. 107-114, 1989.

102. J. F. Ashmore, The Ear's Fast Cellular Motor. *Current Biology*, Vol. 3, pp. 38-40, 1993.

103. J. E. Gale and J. F. Ashmore, Charge Displacement Induced by Rapid Stretch in the Basolateral Membrane of the Guinea-Pig Outer Hair Cell, *Proc. Roy. Soc. B*, Vol. 249, pp. 265-273, 1994.

104. G. D. Housley, D. Greenwood, and J. F. Ashmore, Localization of Cholinergic and Purinergic Receptors on Outer Hair Cells Isolated from the Guinea-Pig Cochlea, *Proc Roy. Soc.* B, Vol. 239, pp. 265-273, 1992.

105. F. Mammano and J. F. Ashmore, Reverse Transduction Measured in the Isolated Cochlea by Laser Michelson Interferometry, *Nature*, Vol. 365, pp. 838-841.